Accretion Disks

Accretion onto Black Holes

Magdalena Karnassnigg

Undergraduate Thesis
Thesis Advisor: Dipl.-Phys. Dr.rer.nat. Thorsten Ratzka
University of Graz
Institute of Physics
Department for Geophysics, Astrophysics and Meteorology

July 2015

Contents

Abstract

The word "accretion" with origin from the Latin "accretio" means to increase or to grow. In an astronomical sense it means an increase of an object's mass by attracting matter due to gravitational force. Accretion disks can be understood as machines which feed the central object with interstellar matter and gas. The feeding generates potential energy and the mass itself is later also transformed into energy. They occur in objects of different scales, such as disks around protoplanetary systems, neutron stars, stellar black holes in binaries and galactic black holes.
For accretion processes to take place, angular momentum transport is required. Only if matter transfers its angular momentum to matter further outside the disk, an inward transport of matter is possible. Instabilities of various kinds cause turbulences in the disk, which ensure angular momentum transport via some kind of turbulent viscosity. The assumed turbulent viscosity enables not just angular momentum transport, but is also a channel for conserving gravitational energy, originating in mass falling onto the central object and transformed into thermal energy. This turbulent viscosity is mentioned in the literature with the so-called α-prescription, which contains in it all the uncertainties that still exist with respect to the origin and properties of this turbulent viscosity. The structure of an accretion disk is dependent on the mass rate that is accreted by the central object, the central star's mass, its angular velocity and the isothermal sound speed. Moreover, a connection between the disk's temperature and its aspect ratio can be found. The internal temperature, that determines the disk's thickness, depends on mechanisms transporting energy to the surface, whereas the surface temperature is dependent on the product $M\dot{M}$. The dissipated energy, during the process of accretion, goes into heat, which is emitted as radiation from the disk's surface and leads to a characteristic spectrum of the disk. Different types of accretion disks, which can be divided into two classes, the geometrically thin and the non-thin disks, have been suggested. The geometrically thin disks contain the steady thin disk, which represents the standard model. Many phenomena in connection with accretion disks have been observed, such as jets. These jets are strongly collimated outflows which occur not in all systems with accretion disks, not all the time respectively. They are assumed to be themselves an electromagnetic phenomena. The magnetic model, in which outflows are produced by magnetic fields of a rotating object, has become the standard for explaining the development of jets. Also different models for explaining the structure, the spectrum and the interaction of disks with their environment have been proposed.
As the structure is dependent on the mass rate, it is obvious to look at objects with high masses for observing these astrophysical phenomena. Therefore black holes in binaries or galactic black holes are great candidates for getting more observational data and greater insight in the physics underlying accretion disks. Measured data from the observation of the center of our Galaxy, Saggitarius A^{*}, has supported the theory of accretion disks, some kind of surrounding matter, respectively.
This thesis does not lay claim of a full summary or representation of the current outcomes in the field of accretion physics neither are all possible models and types of accretion disks presented. The thesis is a summary based on subjective selection of the very most important chapters, following the work of some leading scientists in this sector.

Introduction

Accretion disks have gained more and more interest in astrophysics, initiated with the discovery of a flat solar system, which means that all planets orbit the sun in one plane. Disks are found in star formation processes, accreting binary X-ray sources, black holes and galaxies. They usually play an important role as they determine the emitted radiation from the central object and can reveal processes of planet formation. Besides, they give insight in phenomena like jets and outflows with high X-ray and ultraviolet emission.

Matter falling onto a central massive object cannot be accreted directly as it has angular momentum. Therefore, the matter settles into a flattened rotating configuration, an accretion disk. The process of prime importance is the redistribution of angular momentum inside the disk. Matter nearer the central object transfers angular momentum to the outer parts of the disk and falls onto the star. During this process the disk spreads, which leads to the ultimate goal, to distribute as much angular momentum on as less as possible matter. Generally, an accretion disk is subject to a variety of instabilities, gravitational, magneto-rotational, pure hydrodynamical and convective ones, that, in turn, cause turbulence in the disk, which ensures outward transport of angular momentum. These effects are represented by the so-called turbulent viscosity. However, its origin remains still uncertain. Turbulence plays a dual role in the evolution of an accretion disk, firstly it is necessary for angular momentum transport to take place, second it provides a channel of conversion of gravitational energy, liberated as mass falls onto the star, into thermal energy. The process of angular momentum transport is much slower in systems of larger scale, which encourages amongst other things to see analogies between the present state of the Galaxy and a very much earlier stage of the solar system when it was a spinning disk of gas and dust. Moreover, there exist some interesting connections between disks and outbursts, like jets. Lacking direct observations of disks, different models have been proposed to explain many properties reflected in the emission spectrum. Nevertheless, uncertainty still exists with respect to some basic questions.

This thesis shall give an overall view of the basic equations and considerations, mechanisms and models with respect to accretion disks. The first chapter gives a short introduction and explanation of accretion itself. The second one represents in a more mathematical way the equations describing the structure and shape of an accretion disk, as well as the prime mechanisms inside the disk, such as the angular momentum transport in connection with the turbulent viscosity. Furthermore some models that are useful for describing many phenomena in a wide range of objects are introduced. The last chapter refers to accretion onto black holes. It delineates the definition of the inner rim of an accretion disk around a black hole, the formation of it in a binary system with a stellar black hole and further different types of accretion onto stellar and galactic black holes. Last but not least, recent observational data of our nearest candidate for a galactic black hole, Saggitarius A*, are presented. A table of the used variables and the list of references are given in the appendices.

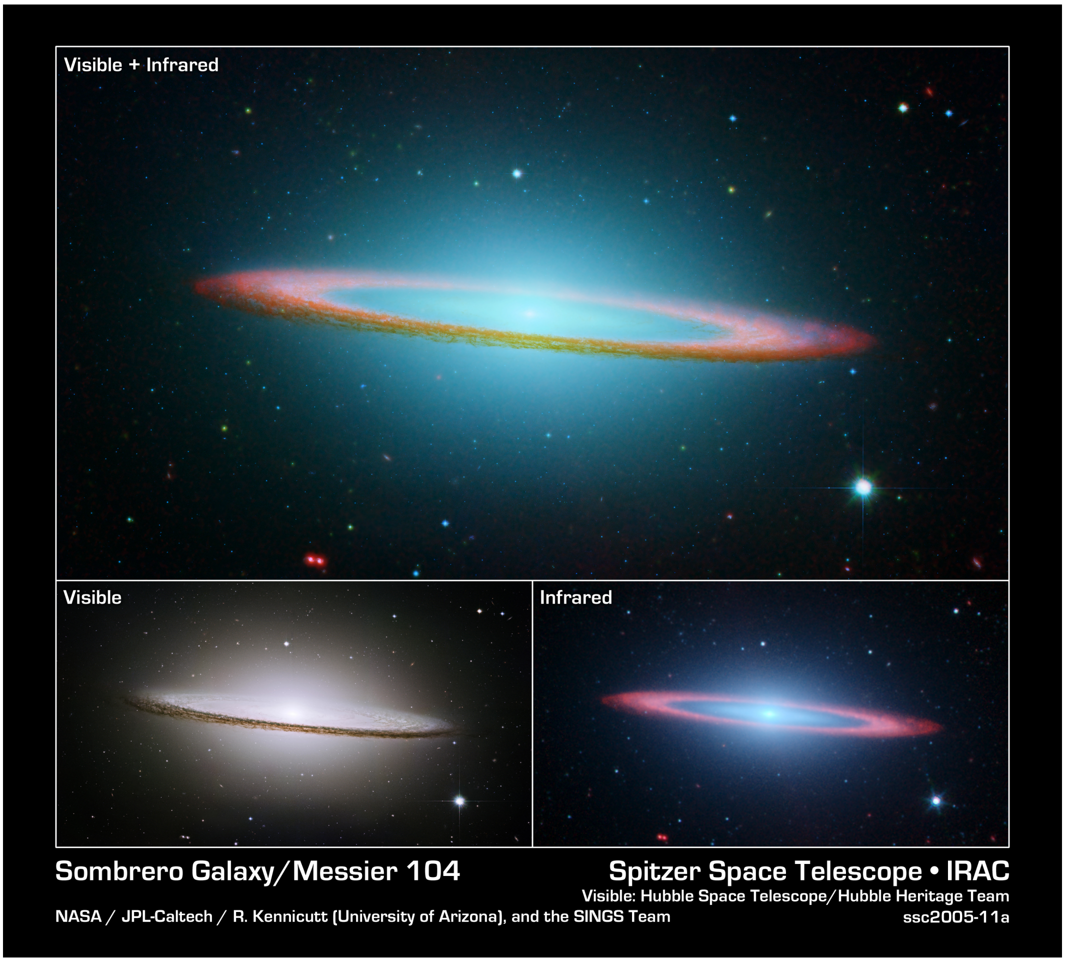

Figure 1: Messier 104, commonly known as the Sombrero Galaxy, in visible and infrared light (NASA/JPL-Caltech and The Hubble Heritage Team (STScI/AURA)).
This picture has been chosen for illustrating the smooth ring of dust around the galaxy and therefore to get an image of an accretion disk around a central mass.
The lower left picture: A visible light image taken by the Hubble space telescope of Messier 104. The observations have been made May-June 2003 with the space telescope's Advanced Camera for Surveys. They were taken with a red, green and blue filter to reveal an image in realistic colors. In this picture only the near rim of the dusty disk can be clearly seen in silhouette.
The lower right picture: A recent image made with Spitzer's infrared array camera, that was able to uncover the bright, smooth ring of dust surrounding the galaxy, seen in red. It is composed of four images, taken at 3.6 (blue), 4.5 (green), 5.8 (orange) and 8.0 (red) μm. (The starlight contribution at 3.6 μm has been subtracted to enhance the visibility of the dust features.) With this image an otherwise hidden disk of stars within the dust ring can be seen. It also reveals that the disk is warped, possibly due to the gravitational encounter of another galaxy. It also shows that there are clumpy areas at the far edges of the ring, which indicates young star forming regions.
The center of this galaxy is supposed to be a super massive black hole, with a mass billion times bigger than our sun.

1 Definition of Accretion

Accretion disks are widespread in objects located in the outer space and are responsible for their interaction with their environment. Lacking the possibility of direct observations, which means spatially resolved observations, a lot of questions with respect to the basic properties and mechanisms remain still open. Although we are already able to resolve such disks around stars via interferometry, however, this is just possible for a few objects.
Accretion means the mechanism of matter accumulation of a central mass due to its gravitational force. During this process angular momentum is transferred from matter of the inner parts to matter further out in the disk, which enables matter to move inward and finally to fall onto the center. In the following the main process is explained with respect to a potential with a point-like central source, based on the work of H.C. Spruit 1996a.

1.1 Fundamental Equations

Gas or matter is falling into a potential ϕ with a point-like central source from a distance r_0 to a distance r and converts gravitational energy into kinetic energy, by an amount of ΔE.

$$\phi = -\frac{GM}{r} \tag{1.1}$$

$$\Delta \mathrm{E} = GMm\left(\frac{1}{r} - \frac{1}{r_0}\right) \tag{1.2}$$

Using the gravitational constant G and the central object's mass M. If we assume a large initial distance ($r_0 \to \infty$) the equation simplifies to $\Delta \mathrm{E} = GMm/r$. Further two cases for the amount of energy dissipated per unit mass can be distinguished.

Case 1: If the gas is brought to rest, for instance on the surface of the star.

$$e = \frac{GM}{r} \tag{1.3}$$

Case 2: If the gas goes into a circular Kepler orbit. The dissipated energy goes into internal energy of the gas and radiation, which escapes, usually in the form of photons, to infinity.

$$e = \frac{1}{2}\frac{GM}{r} \tag{1.4}$$

If radiation losses are neglected adiabatic accretion takes place.[1] Therefore the internal energy per unit mass for an ideal gas with constant ratio of specific heat is given by

$$e = \frac{P}{(\gamma - 1)\rho}\ . \tag{1.5}$$

[1] That is the case when the gas is accreted and therefore only if the gas does not go into a Keplerian orbit.

Using the equation of state $P = \mathcal{R}\rho T/\mu$ for an ideal gas, the specific heat γ, the universal gas constant $\mathcal{R}$, T as the temperature, the gas density ρ and the mean atomic weight per particle μ.

Assuming the second case 1.4, that the gas is going into a circular orbit, the temperature of the gas after the dissipation has taken places, is given by

$$T = \frac{1}{2}(\gamma - 1)T_{\mathrm{vir}} \ , \tag{1.6}$$

defining the virial temperature as

$$T_{\mathrm{vir}} = \frac{GM\mu}{\mathcal{R}r} \ . \tag{1.7}$$

As the speed of sound ($c_{\mathrm{s}} = (\gamma\mathcal{R}T/\mu)^{1/2}$) is dependent on the temperature, in an atmosphere with temperature near T_{vir} the speed of sound is close to the escape speed ($v_{\mathrm{esc}} = \sqrt{2GM/r}$) from the system. Such an atmosphere may evaporate on a relatively short time scale in the form of a stellar wind. The larger γ the larger the temperature in the accreted gas. Beyond a critical value of γ the temperature is too high for the gas to stay bound in the potential. The adiabatic spherical accretion takes place on the dynamical or free fall time scale

$$\tau_{\mathrm{d}} = \frac{1}{\Omega_{\mathrm{k}}} = \frac{r}{v_{\mathrm{k}}} = \sqrt{\frac{r^3}{GM}} \ . \tag{1.8}$$

Using the Keplerian orbital velocity $v_{\mathrm{k}} = \sqrt{GM/r}$ and the Keplerian angular velocity $\Omega_{\mathrm{k}} = \sqrt{GM/r^3}$, G, M and r as mentioned above.

When radiative losses are not neglected and become important the accreting gas can stay cool irrespective of the value of γ. Usually the temperatures of accretion disks are much lower than the virial temperature. It should be noted that the optical depth of the disk increases with the accretion rate $\dot{M}$. When the optical depth becomes large enough to trap the photons in the flow, the accretion carries them inside the disk, together with the gas, towards the central mass. Therefore above a critical rate, $\dot{M}_{\mathrm{c}}$, accretion is adiabatic.
According to the accretion rate, critical values for the disk's luminosity as well as for the disk's flux can be defined. Outward traveling photons are scattered or absorbed and exert a radiative force. In objects with high luminosity this radiative force has the tendency to blow their atmospheres away. During this process two forces occur. The force caused by the radiative flux $F\kappa/c$ and the force of gravity pulling back on the mass, GM/r^2.[2] The critical flux is defined as the flux at which both forces are in balance, the Eddington flux

$$F_{\mathrm{E}} = \frac{c}{\kappa}\frac{GM}{r^2} \tag{1.9}$$

with c the speed of light. Assuming the flux to be spherical symmetric, a critical luminosity, the Eddington luminosity L_{E} can be defined.

$$L_{\mathrm{E}} = 4\pi GM\frac{c}{\kappa} \tag{1.10}$$

Assuming the gas to be fully ionized, its opacity is dominated by electron scattering, and for solar composition κ is of the order of $0,3\ \mathrm{cm}^2/\mathrm{g}$. Therefore L_{E} can be written like [3]

[2] This equations apply to one gram of matter and a scattering or absorbing surface area of $[\kappa] = \mathrm{cm}^2$ to the escaping radiation. [3] The sign $\odot$ refers to the physical quantities with respect to the sun.

$$L_{\mathrm{E}} \approx 1,7 \cdot 10^{38} \frac{M}{M_{\odot}} \text{ erg/s} \approx 4 \cdot 10^{4} \frac{M}{M_{\odot}} L_{\odot}. \tag{1.11}$$

Furthermore an Eddington accretion rate can be derived

$$\frac{GM}{r} \dot{M}_{\mathrm{E}} = L_{\mathrm{E}} \rightarrow \dot{M}_{\mathrm{E}} = 4\pi r \frac{c}{\kappa}. \tag{1.12}$$

It is important to mention that the Eddington luminosity is a true limit which can not be exceeded (by a statically radiating object, except by geometrical factors of order unity), whereas no maximum exists according to the Eddington accretion rate. Assuming an accretion rate $\dot{M} > \dot{M}_{\mathrm{E}}$, all the plasma including the radiation energy is just swallowed.

2 Accretion Disks

2.1 Structure/Thickness

2.1.1 Geometrical Thickness

The discussion in this subsection is based on the work of Spruit 1996a.
To derive a disk's thickness one must find its equilibrium in the direction perpendicular to the disk plane, in the z direction. Assuming an axis symmetric disk, using cylindrical polar coordinates (r, ϕ, z) and measuring the forces at a point $\mathbf{r}_0(r, \phi, z)$ in a co-rotating frame with the Keplerian angular velocity Ω_k, the gravitational acceleration is given by $-GM/r^2\ \hat{\mathbf{r}}$ and the centrifugal acceleration by $\Omega_\mathrm{k}^2\mathbf{r}$. ($\hat{\mathbf{r}}$ defines a unit vector in the spherical radial direction r.[4]) The residual acceleration toward the mid-plane by expanding both accelerations near $\mathbf{r}_0$ is given by:

$$g_\mathrm{z} = -\Omega_\mathrm{k}^2 z \tag{2.1}$$

A hydrostatic density distribution under this acceleration, by assuming an isothermal gas, can be deduced

$$\rho = \rho_0(r) \exp\left(-\frac{z^2}{2H^2}\right) . \tag{2.2}$$

With the used variables ρ as the hydrostatic density, $\rho_0(r)$ the density at the mid-plane, the z direction and H, the scale height. The scale height $H(r)$ can be written as function of the isothermal sound speed c_s, see Definition of Accretion

$$H = \frac{c_\mathrm{s}}{\Omega_\mathrm{k}} . \tag{2.3}$$

The aspect ratio of the disk can be written in various ways:

$$\delta = \frac{H}{r} = \frac{c_\mathrm{s}}{\Omega_\mathrm{k} r} = \left(\frac{T}{T_\mathrm{vir}}\right)^{1/2} . \tag{2.4}$$

For the moment we are ignoring viscosity and derive the equation of motion in the potential of a point like mass.

$$\frac{\partial \mathbf{v}}{\partial t} + \mathbf{v} \cdot \nabla \mathbf{v} = -\frac{1}{\rho} \nabla P - \frac{GM}{r^2} \hat{\mathbf{r}} . \tag{2.5}$$

Using $\mathbf{v}$ the velocity, ∇P the pressure gradient, G the gravitational constant, M the object's mass and $\hat{\mathbf{r}}$ as defined above. More detailed, the pressure gradient term is

[4] In the following and above, the bold font stands for vectors.

$$\frac{1}{\rho}\nabla P = \frac{\mathcal{R}}{\mu} T \nabla \ln P \ . \tag{2.6}$$

If cooling is important, the pressure gradient term is negligible, which is equivalent to the assumption that the gas moves hypersonically on nearly Keplerian orbits. (Using dimensionless quantities $\tilde{r} = r/r_0, \tilde{v} = v/(\Omega_0 r_0), \tilde{t} = \Omega_0 t, \tilde{\nabla} = r_0 \nabla$, the equation of motion goes into $-T/T_{\text{vir}} \tilde{\nabla} \ln P - 1/\tilde{r}^2 \hat{\mathbf{r}}$ and the coefficient of the pressure gradient term is $T/T_{\text{vir}} \ll 1$ if cooling is important.)

2.1.2 Optical Thickness

The released energy through viscous dissipation from the gravitational potential energy can move inward with the matter or can be emitted by radiative cooling processes in the vertical direction to the disks plane. The efficiency of such cooling processes is more or less dependent on the optical depth of the disk. One discriminates between the optical thick case (where the optical depth $\tau \gg 1$) and the optical thin case ($\tau \ll 1$). This differentiation is dependent on the observation frequency. The further discussion is based on the work of D. Asmus 2008.

Optical Thick Case

In the case of a high opacity of the disk, the emitted photons are constantly absorbed and re-emitted or scattered on there way outside. The average path length is much smaller than the vertical expansion of the disk. Assuming the Thomson scattering on free electrons to be the dominant process, which can only be assumed if almost all of the matter is fully ionized (plasma), a radiative emission rate per unit area can be found

$$q^-_{\text{thick}} = \frac{2acT^4}{3\kappa\rho h^2} \ . \tag{2.7}$$

$a = 4\sigma_{\text{SB}}/c$ refers to the radiation constant, σ_{SB} the Stefan-Boltzmann constant, h represents the half thickness of the disk, $H/2$, and κ the opacity. In the optical thick case a radiation pressure ($p_{\text{rad}} = (a/3)T^4$) occurs, which must be added to the total pressure.

Optical Thin Case

The average path length of the photons is bigger than h, which means a photon is usually able to escape the disk without absorption and re-emission, or scattering. The emitted energy is strongly dependent on the observed physical processes and a detailed description would need a separate treatment of electrons and ions. We can approximate it, however, by two assumptions. For both it is required that the gas can be described through an equation of state and temperature and the radiation pressure can be neglected.

- The density is so low that the occurring cooling can be neglected, as there is too less interaction. This means that the heat factor ($f(r)$), which measures the efficiency of radiative cooling, of the whole disk is constant (see 2.5.2). q^+ and q^- refer to the height integrated viscous dissipation rate and the radiative loss rate and are given in equation 2.76.

$$f(r) = \text{const.} \qquad \longleftrightarrow \qquad q^- \propto q^+ \tag{2.8}$$

- The gas is only cooled through thermal bremsstrahlung, given through:

$$q^{-}_{\text{brak}} = -1,24 \cdot 10^{21} \rho^2 T^{1/2} \frac{\text{erg}}{\text{s cm}^3}. \tag{2.9}$$

2.2 Angular Momentum Transport/ Viscosity

In many cases the accreting gas has a non-zero angular momentum and therefore can not be accreted directly. Only if matter transfers its angular momentum to matter further out in the disk, an inward transport of matter is possible.[5] This principle of distributing as much angular momentum on as little as possible matter is the main definition of accretion (Asmus 2008). The result of this asymmetric behavior is, that almost all the mass of a disk can be accreted, without an external torque removing the angular momentum. Usually disks are subjects to gravitational, magnetorotational (MRI), purely hydrodynamical and convective instabilities that, in turn, cause turbulence in disks which ensures outward transport of angular momentum. This effect of turbulence can be characterized as turbulent viscosity. The dual role of turbulence shall be mentioned. Firstly, it is responsible for outward angular momentum transport, secondly, it provides a channel for conserving gravitational energy, originating in mass falling onto the central object and transformed into thermal energy. This dissipated energy, in turn, can be measured and observed as it contributes to the emitted radiation. The further steps and equations including the subsection Evolution of the Disk's Viscosity are based on the work of G. (Mamatsashvili 2011)

For a more specific explanation we are assuming the simplest disk model: a central object of large mass M surrounded by a razor thin gaseous accretion disk. The approximation of a razor thin disk means that the scale height $H = c_{\text{s}}/\Omega_{\text{k}}$ is much smaller than the distance from the central star $H/r \ll 1$. This is equivalent to the requirement that the speed of sound c_{s} is much lower than the rotation velocity $v_{\text{k}} = r\Omega_{\text{k}}$, or in other words the disk is supersonic. Using again cylindrical polar coordinates (r, ϕ, z), with the central mass in its origin and the disk at the $z = 0$ plane, basic hydrodynamic equations are integrated in the vertical direction and therefore yield to two-dimensional equations. The disk is then characterized by its surface density Σ

$$\Sigma = \int_{-\infty}^{\infty} \rho \, dz \approx 2H_0\rho_0. \tag{2.10}$$

The approximation on the right side is used to clarify that the coefficient in front of H_0 is dependent on details of the vertical structure of the disk. The disk being accreting means that there is also a radial or „drift" velocity v_{r} towards the central object. This „drift" velocity is much smaller than the orbital velocity v_{k} and the quantities can be ordered like this: $v_{\text{r}} \ll c_{\text{s}} \ll v_{\text{k}} = r\Omega_{\text{k}}$ implying that accretion takes place on a longer time scale than the dynamical time τ_{d}. Due to the fact that we assume the disk to be axis-symmetric all variables are only functions of r and time t, so by integrating the continuity equation over z the conservation of mass in terms of the surface density $\Sigma(r,t)$ is

$$\frac{\partial \Sigma}{\partial t} + \frac{1}{r}\frac{\partial}{\partial r}(r\Sigma v_{\text{r}}) = 0. \tag{2.11}$$

The former ordering of the velocities is directly linked with the viscosity parameter ν, so we can find another equation in a similar way for describing the angular momentum conservation.

[5] As the orbits are close to Keplerian, a change in angular momentum of a ring of gas also means it must change its distance from the central object. So in a thin disk this implies a redistribution of mass in the disk.

$$\frac{\partial}{\partial t}(\Sigma r^2\Omega) + \frac{1}{r}\frac{\partial}{\partial r}(r\Sigma v_{\mathrm{r}} r^2\Omega) = \frac{1}{r}\frac{\partial}{\partial r}(\nu\Sigma r^3\Omega') \tag{2.12}$$

Viscous forces are now included proportional to ν and the prime with Ω defines a derivation with respect to r. A single equation for the evolution of the surface density can be derived by combining 2.11 and 2.12.

$$\frac{\partial\Sigma}{\partial t} = \frac{3}{r}\frac{\partial}{\partial r}\left[r^{1/2}\frac{\partial}{\partial r}(\nu\Sigma r^{1/2})\right] \tag{2.13}$$

This equation can be understood as the basic equation of the time-dependent surface density, or mass transport, relating it to some kind of viscosity, parameterized by ν in a Keplerian disk. It is the *standard thin disk diffusion equation*. As ν is not necessarily constant and can be a very complex function of local variables, such as temperature, radius, surface density and ionization fraction, 2.11 is a non-linear diffusion-type equation for Σ. Therefore, this equation should be solved numerically, but if it can be expressed as a power of radius, an analytic solution is possible (Lynden-Bell and Pringle 1974). Using this simplification one can get a general feeling for angular momentum evolution. Estimates can be made with regard to the radial velocity, 2.14, and the typical timescale of viscous/secular evolution, 2.15.

$$v_{\mathrm{r}} = -\frac{3}{\Sigma r^{1/2}}\frac{\partial}{\partial r}(\nu\Sigma r^{1/2}) \sim \frac{\nu}{r} \tag{2.14}$$

$$\tau_{\mathrm{visc}} \sim \frac{r}{v_{\mathrm{r}}} \sim \frac{r^2}{\nu} \tag{2.15}$$

Further, the energy dissipation rate, the heat produced during the accretion process, can be derived per unit area, per unit time at some r.

$$Q(r) = \frac{1}{2}\nu\Sigma(r\Omega')^2. \tag{2.16}$$

This heat originates from the gravitational energy released from the infalling matter.
The here presented analysis shows that viscosity is an important parameter for disk evolution and is mainly responsible for the outward transport of angular momentum. However, we just introduced ν in 2.12 without detailed description, since it is one of the major unresolved questions. Standard molecular viscosity is far too small and therefore the viscous time scale too big for getting appropriate timescales compared with observed disk lifetimes. Estimates for protoplanetary disks show that the Reynolds number is around 10^{14}.[6] The dynamical time scale for protoplanetary disks is of the order of a few years, so the viscous time scale would be of the age of the universe. This predicts that there must be another kind of mechanism or some kind of anomalous viscosity producing time scales of orders of magnitude smaller. From laboratory experiments it is known that there is a critical value of the Reynolds number around $10^3 - 10^4$, if it is gradually increased, after which the flow becomes turbulent. After this critical value the velocity undergoes large and chaotic variations on random short time and length scales. When a disk's Reynolds number is compared with its threshold values in laboratory experiments, scientists assume disk flows to be turbulent as well. This turbulent flow will be characterized by the size of the turbulent eddies λ_{t} and the turnover velocity v_t of the largest eddies and therefore the turbulent viscosity can be defined

[6] The Reynolds number is given as the ratio of viscous and dynamical times by $\tau_{\mathrm{visc}}/\tau_{\mathrm{d}} \sim r^2/(H\lambda) \sim Re$, it quantifies the relative importance of inertial forces to viscous forces for given flow conditions. The mean free path for a typical protoplanetary disk is $\lambda \sim 1/n\sigma = 2,5$ cm, using for the number density $n \sim 4 \cdot 10^{14}$ cm^{-3} of molecules and for cross-section $\sigma \sim 10^{-15}$ cm^2, for $H/r \sim 0,05$ and $r \sim 1$ AU for the radius.

as $\nu = \lambda_{\mathrm{t}} v_{\mathrm{r}}$. As we assume λ_{t} to be of order magnitude larger than the mean free path, ν becomes larger too and can provide anomalous transport of angular momentum.
Unfortunately, yet the underlying physical mechanisms causing the transition to turbulence in disks is not exactly known, and so the sizes and velocities of eddies neither. Investigations in the last two decades have shown that viscosity induced by turbulence mostly originates in magnetorotational and gravitational instabilities, possibly convective instabilities as well. Former estimates on their hydrodynamic origin has been falsified, as many studies have shown that Keplerian differential rotation of a gas in the absence of magnetic fields and self-gravity is stable linearly and nonlinearly. Although the origin of turbulent viscosity is not clarified, the typical size of the largest eddies λ_{t} and the turnover velocity v_{r} can be characterized. λ_{t} can not exceed the disk's thickness, otherwise turbulence would not be isotropic and would not transport locally, so $\lambda_{\mathrm{t}} < H$. Moreover, it is unlikely that turbulences in disks are supersonic, otherwise strong shocks would appear and damp turbulences to subsonic values, so $v_{\mathrm{t}} < c_{\mathrm{s}}$. Using these two predictions, (Shakura and Sunyaev 1973) suggested a prametrization for turbulent viscosity:

$$\nu = \alpha c_{\mathrm{s}} H. \tag{2.17}$$

Here α refers to a constant, usually less than unity and contains in itself all the uncertainties regarding the mechanism and properties of turbulences in disks. In only one parameter two of the most important mechanisms of angular momentum transport, the magnetic field and turbulence, are characterized. This formula is known as the α-prescription or α-parametrization of turbulent viscosity.
The value of α can be specified: if turbulent mechanisms are present $\alpha < 1$. For $\alpha > 1$ turbulence must be supersonic and would lead to a rapid heating of the plasma and therefore to $\alpha \leq 1$. It is likely that for magnetic transport $\alpha < 1$, further for typical initial conditions it is likely that $\alpha \ll 1$, as assumed in many cases. α is a function of R and in a wide range the structure of the disk is not essentially changed (Shakura and Sunyaev 1973).

$$10^{-15}\left(\frac{\dot{M}}{\dot{M}_{\mathrm{E}}}\right)^2 < \alpha < 1 \tag{2.18}$$

The left side of the equation links the α-prescription with the ratio of matter inflow into the disk. The structure and spectrum of the disk depend on the matter inflow $\dot{M}$ and therefore as well the α-viscosity.

2.2.1 Evolution of the Disk's Viscosity

Constant Viscosity

Assuming the simplest case of spatial uniformity, ν is constant. Then 2.13 can be rewritten:

$$\frac{\partial}{\partial t}(r^{1/2}\Sigma) = \frac{3\nu}{r}\left(r^{1/2}\frac{\partial}{\partial r}\right)^2 (r^{1/2}\Sigma). \tag{2.19}$$

By substituting $s = 2r^{1/2}$ and $\mathrm{d}s/\mathrm{d}r = r^{-1/2}$ one gets:

$$\frac{\partial}{\partial t}(r^{1/2}\Sigma) = \frac{12\nu}{s^2}\frac{\partial^2}{\partial s^2}(r^{1/2}\Sigma). \tag{2.20}$$

Separating variables using $r^{1/2}\Sigma = T(t)S(s)$ we get:

$$\frac{T'(t)}{T(t)} = \frac{12\nu}{s^2}\frac{S''(s)}{S(s)} = const. \tag{2.21}$$

T and S are exponential and Bessel functions.[7] Finding Green's function, taking as the initial matter distribution a ring of mass m at $r = r_0$, we find a solution for the surface density $\Sigma(r,t)$. Using standard models and again dimensionless variables, $\tilde{r} = r/r_0$ and $\tilde{t} = 12\nu t/r^2$, one gets 2.22 with the modified Bessel function $I_{1/4}(z)$:

$$\Sigma(\tilde{r},\tilde{t}) = \frac{m}{\pi r_0^2}\tilde{t}^{-1}\tilde{r}^{-1/4}\exp\left(-\frac{1+x^2}{\tilde{t}}\right) I_{1/4}(2x/\tilde{t}). \tag{2.22}$$

Using 2.14 and knowing Σ (still with $\nu =$ const) the radial velocity can be defined and therefore the mass inflow into the center:

$$v_\mathrm{r} = -3\nu\frac{\partial}{\partial r}\, ln(r^{1/2}\Sigma) = -\frac{3\nu}{r_0}\frac{\partial}{\partial\tilde{r}}\ln(\tilde{r}^{1/2}\Sigma) = \tag{2.23}$$
$$-\frac{3\nu}{r_0}\frac{\partial}{\partial\tilde{r}}\left(\frac{1}{4}\ln\tilde{r} - \frac{1+\tilde{r}^2}{\tilde{t}} + \ln I_{1/4}\left(\frac{2\tilde{r}}{\tilde{t}}\right)\right).$$

As the modified Bessel function $I_{1/4}(z)$ shows an asymptotic behavior, $I_{1/4}(z) \propto z^{-1/2}e^z$ at $z \gg 1$ and $I_{1/4}(z) \propto z^{1/4}$ at $z \ll 1$, one can distinguish two cases for the radial velocity

$$v_\mathrm{r} \sim \frac{3\nu}{r_0}\left(\frac{1}{4\tilde{r}} + \frac{2\tilde{r}}{\tilde{t}} - \frac{2}{\tilde{t}}\right) > 0, \quad at\ 2\tilde{r} \gg \tilde{t}, \tag{2.24}$$

$$v_\mathrm{r} \propto -\frac{3\nu}{r_0}\left(\frac{1}{2\tilde{r}} - \frac{2\tilde{r}}{\tilde{t}}\right) < 0, \quad at\ 2\tilde{r} \ll \tilde{t}. \tag{2.25}$$

Because of that the outer parts of the matter distribution move outwards, taking with them the angular momentum of the matter in the inner parts that moves inward towards the central mass. It is also important that the radius at which v_r changes its sign also moves outwards. Parts which are initially located at $\tilde{r} \gg \tilde{t}$ are changing to $\tilde{r} \ll \tilde{t}$ after sufficient time. So parts who are at radii $r > r_0$ firstly move to larger radii, but then begin to lose angular momentum to parts still larger and are forced drifting inwards. After a long time ($\tilde{t} \gg 1$) almost all mass is accreted by the central object and almost all of the angular momentum is located at very large radii, where only a small fraction of the initial mass resides.

Radially Varying Viscosity

Considering now a more complex viscosity, ν is given as a function of r:

$$\nu = \nu_0\left(\frac{r}{r_0}\right)^\gamma \equiv c_0 r^\gamma. \tag{2.26}$$

Substituting again, here with $h = r^{1/2}$ and $g = \nu\Sigma r^{1/2}$, 2.13 can be written as:[8]

[7] They are the canonical solutions of Bessel's differential equation. [8] Here h and g are only free parameters used for the subsitution and h does not refer to the half thickness of the disk.

$$\frac{\partial^2 g}{\partial h^2} = \frac{4h^{2(1-\gamma)}}{3c_0}\frac{\partial g}{\partial t}. \tag{2.27}$$

Further we get

$$\frac{\partial^2 g}{\partial h^2} + \frac{4sh^{2(1-\gamma)}}{3c_0} g = 0 \tag{2.28}$$

or

$$\frac{d^2 g_1}{dx^2} + \frac{1}{x}\frac{dg_1}{dx} + \left(\frac{4s}{3c_0} - \frac{1}{4x^2}\right)\frac{g_1}{(\gamma-2)^2} = 0, \tag{2.29}$$

when using for the time variation $g \propto e^{-st}$ and setting $x = h^{2-\gamma}$ and $g_1 = x^{1/2(\gamma-2)}g$. For getting a more precisely understanding of the time-dependent solution of Bessel's differential equation, we first look at a special solution from the initial distribution of g:

$$g(h,0) = Ch \cdot \exp(-ah^{2(2-\gamma)}) = Cx^{1/(2-\gamma)}\exp(-ax^2). \tag{2.30}$$

C and a are some positive constants. As g should vanish at large distances, we assume $\gamma < 2$ and find an analytic solution:

$$g(x,t) = CT^{-\frac{(2\gamma-5)}{2(\gamma-2)}} x^{1/(2-\gamma)} \exp(-ax^2/T) \tag{2.31}$$

or

$$g(h,t) = CT^{-\frac{2\gamma-5}{2(\gamma-2)}} h \cdot \exp(-ah^{2(2-\gamma)}/T)$$

where $T = 1 + 3act(\gamma-2)^2$ is a dimensionless time. Substituting the partial differential of 2.14 by an absolute differential with a coefficient, we get a new solution for the radial velocity:

$$\begin{aligned} v_\mathrm{r} &= -\frac{3}{2\Sigma h^2}\frac{dg}{dh} = \left|\Sigma = \frac{g}{h\nu} = \frac{g}{ch^{2\gamma+1}}\right| = -\frac{3ch^{2(\gamma-a)}}{2g}\frac{dg}{dh} \\ &= -\frac{3ch^{2(\gamma-1)}}{2}\left(1 - \frac{2(2-\gamma)ah^{2(2-\gamma)}}{T}\right) \end{aligned} \tag{2.32}$$

Taking a look at this equation we see that the radial velocity is directed outwards for $h > (T/2a(2-\gamma)^{1/2(2-\gamma)}$ and vice versa. This point moves out, with increasing T and overtakes more and more matter and we find the same result as in subsection Constant Viscosity. Almost all of the matter follows an inward drift towards the center and a little fraction of matter carries the bulk of angular momentum. So the conclusions of these investigations are that the total amount of angular momentum within a fixed radius r decreases with time, as it flows outwards. The total mass of the disk decreases as $T^{-1/2(2-\gamma)}$. This decrease of the total mass of the disk is understood as the mass flux into the origin, therefore the real matter distribution is a growing central point mass surrounded by a density distribution which grows in size, but decreases in mass. Hence, considering material that starts inside the point of radial velocity reversal will move inward, whereas matter starting outside will begin moving outwards to be overtaken. Once overtaken it will start moving inwards and ends likewise at $r = 0$. For this considered case the special angular momentum h is given by $h = \Omega_\mathrm{k} r^2 \propto r^{1/2}$ and hence tends to infinity at large radii.

2.2.2 Sources of Viscosity

The discussion in this subsection, including Magnetic Viscosity and Radiation-Supported Disks and Viscosity refers to the work of H.C. Spruit 1996a.
Following 2.2 many physicists argue that the high Reynolds number occurring in accretion disks is not a sufficient reason for the presence of hydrodynamic turbulences in the flow. It is mentioned that the gas moving on quite stable Keplerian orbits would also affect the turbulence, as this rotation would have a stabilizing effect on turbulences. Further arguments are that such hydrodynamic turbulences would produce an α which is not dependent on the disk's nature, and therefore α would have the same value in all disks. This case is unlikely as some models show that α increases with temperature. As in many cases the only possibility for getting some insight in the nature of the turbulences is the use of 3-D numerical simulation. Yet these simulations have not shown the estimated hydrodynamic turbulences. Since the attempt to find a fitting solution has not been fruitfully yet, physicists endeavor finding some other plausible mechanisms explaining high Reynolds numbers and the source of viscosity. Some of the proposed mechanisms include convection due to a vertical entropy gradient or waves of various kinds. Such waves would not act locally but globally, as they would effectively transport angular momentum outwards by traveling inwards and dissipating there. One solution of this waves would be spiral shocks, which would produce in hot disks an effective α of 0.01, but are not very likely in cool disks. Another suggested mechanism is based on magnetically accelerated winds, originating from the disk's surface. In fact, such disks could explain the angular momentum loss to make accretion possible if viscosity, due to hydrodynamic turbulences, is not present. Moreover, magnetically accelerated winds would be a good explanation for many outflows and jets, observed in protostellar objects and AGNs (Active Galactic Nuclei). Another possibility are selfgravitating instabilities of the disk. It is assumed that these cause internal friction in sufficiently cool or massive disks.

Magnetic Viscosity

As mentioned above magnetic forces can be very effective in transporting angular momentum outwards. Numerical solutions have shown that in sufficiently ionized disks the shear flow produces some kind of a small scale fast dynamo process (which is indeed a kind of magnetic turbulence) in the disk. In this small scale magnetic field the azimuthal component dominates and the angular momentum transport happens due to magnetic stresses, whereas the fluid motion due to the magnetic forces has little influence on the mechanism. These considerations and numerical solutions have also shown that the development of a small initial field through magnetic shear instability is possible in a perfectly conductive plasma, and therefore that strong accretion flows must be magnetic.

Radiation-Supported Disks and Viscosity

This subsection refers to a special type of accretion explained in more detail in Radiation Supported-Radiatively Inefficient Accretion. The radiation pressure must be taken into account and added to the gas pressure, therefore the total pressure is higher than normal. If the viscosity scales with $\nu = \alpha c_{\mathrm{s}}^2/\Omega$, it turns out that the disk is locally unstable. An increase in temperature would cause an increase of the radiation pressure, which in turn increases the viscous dissipation and again the temperature. This runaway has opened the question whether the radiation pressure should be included in the viscosity in the calculation of the speed of sound or not. However, it has been shown that in case of stresses due to magnetic turbulences the speed of sound most likely scales with the gas pressure alone. As the possibility for magnetic stresses is likely, it is reasonable to scale the effective viscosity in radiation supported disks with the gas pressure $\nu \sim \alpha P_{\mathrm{g}}/(\rho\Omega)$.

2.3 Temperature - Emitted Radiation

> The surface temperature of the disk, which determines how much energy it loses by radiation, is governed primarily by the energy dissipation rate in the disk, which in turn is given by the accretion rate.[1]

In other words, the dissipated energy goes into heat, that is emitted as radiation from the disk's surface. Firstly, the emitted spectrum must be determined locally at each point in the disk and afterwards one can find the disk's entire radiation spectrum by integration. Assuming the disk to be optically thick, which means that every point radiates like a black-body with $T(r)$, the corresponding temperature distribution simplifies. This distribution is found by equating the dissipation rate $Q(r)$ per unit area to the energy flux for a blackbody. Starting from the first law of thermodynamics and integrating over z we get (following the discussion of H.C. Spruit 1996a)

$$\rho T \frac{dS}{dt} = -\, div\mathbf{F} + Q(r), \tag{2.33}$$

$$2\sigma_{\mathrm{SB}} T_{\mathrm{s}}^4(r) = \int\limits_{-\infty}^{\infty} Q(r)\; dz. \tag{2.34}$$

Defining as ρ the density, S the entropy per unit mass, F the heat flux, $Q(r)$ the dissipation rate, i.e. the energy flux, radiated from the surface of the disk, $\sigma_{\mathrm{SB}} = a_{\mathrm{r}} c/4$ Stefan-Boltzmann's constant, with a_{r} the radiation density constant, and as $T_{\mathrm{s}}(r)$ the surface temperature. So the divergence turns into a surface term and the factor 2 represents the 2 radiating surfaces of the disk, which are assumed to radiate like blackbodies.[9]

$$Q(r) = \sigma_{\mathrm{SB}} T_s^4(r) = \frac{3GM\dot{M}}{8\pi r^3}\left[1 - \left(\frac{r_*}{r}\right)^{1/2}\right] \tag{2.35}$$

$$\left|\text{with } \; r \gg r_* \;\&\; T_* = \left(\frac{3GM\dot{M}}{8\pi\sigma_{\mathrm{SB}} r_*^3}\right)^{1/4}\right| \rightarrow T_s(r) = T_* \left(\frac{r_*}{r}\right)^{-3/4} \tag{2.36}$$

Using r_* and T_*, the stellar radius and the characteristic blackbody temperature of the star. Here we can already see that the surface temperature is not dependent on the very uncertain viscosity ν, but only on the product $M\dot{M}$. It should be clarified that 2.36 only represents the surface temperature of the disk, an approximation for the internal temperature will be made in the following and depends on mechanisms transporting energy to the surface. This transport determines in turn the disk's thickness. Therefore, the vertical structure of the disk must be calculated.

After calculating the surface temperature $T_{\mathrm{s}}(r)$, the emitted spectrum by each element of area of the disk can be quantified. In the following equations, which are based on the work of G. Mamatsashvili 2011, ϑ refers to the frequency. Please keep in mind, we are neglecting here the atmosphere of the disk. (i.e. the part of the disk material at optical depth $\tau \leq 1$) Assuming an observer at a distance d whose line of sight forms an angle ψ with the disk plane, the flux at frequency ϑ can be derived. (Here ϑ is used for the frequency as ν is already used for the turbulent viscosity.) Using again the blackbody assumption leads to 2.39.

---

[1] Spruit 1996a, p. 23. [9] Making these calculations, it has been assumed that the disk extends all way down to the surface $r = r_*$ of the central star.

$$I_\vartheta = B_\vartheta[T_\mathrm{s}(r)] = \left| B_\vartheta = \frac{2h\vartheta^3}{c^2} \frac{1}{e^{\frac{h\vartheta}{kT_\mathrm{s}(r)}} - 1} \right| = \frac{2h\vartheta^3}{c^2(e^{h\vartheta/kT(r)-1})} \tag{2.37}$$

$$S_\vartheta = \frac{2\pi\cos(\psi)}{d^2} \int_{r_*}^{r_\mathrm{out}} I_\vartheta r \, dr \tag{2.38}$$

$$S_\vartheta = \frac{4\pi h\cos(\psi)\vartheta^3}{c^2 d^2} \int_{r_*}^{r_\mathrm{out}} \frac{r \, dr}{e^{h\vartheta/kT_\mathrm{s}(r)-1}} \tag{2.39}$$

I_ϑ is the emitted spectrum by each element of area, B_ϑ the Planck-Function, noted in 2.37, r_out is the outer radius of the disk, r_* the stellar radius, h the Planck constant, k Boltzmann's constant, c the speed of light, S_ϑ the flux at frequency ϑ. In the figure below the integrated spectrum of a steady accretion disk is illustrated.

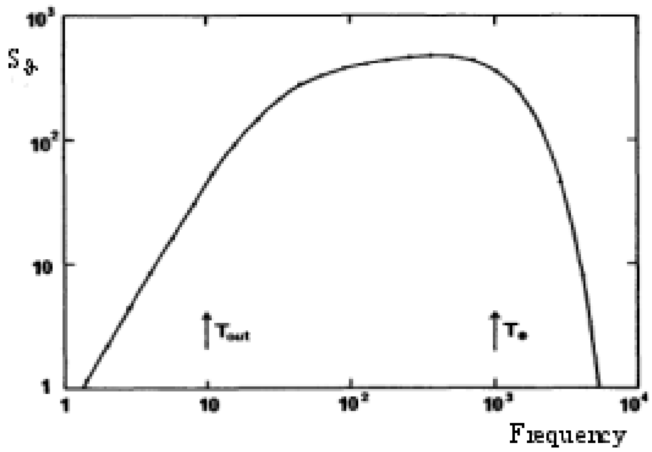

Figure 2.1: Integrated spectrum of a steady disk: A local blackbody spectrum is radiated at each point. It is a shematic illustration with arbitrary units. Frequencies are shown for the disks outermost temperature T_out and the characteristic inner temperature T_*. (Mamatsashvili 2011, p. 10)

This formula is independent of the viscosity ν, which is a consequence of the steady and blackbody assumption. 2.39 is at least a crude representation of the observed spectrum for some systems.

The following considerations are based on the work of H.C. Spruit 1996a.
Now we will make an approximation for the temperature *in* the disk. In the plane or more generally in stellar interiors, energy transport happens due to radiation processes rather than to convective ones at high temperatures. Assuming local thermodynamic equilibrium the temperature structure of a radiative atmosphere in the Eddington approximation[10] can be written as

$$\frac{d}{d\tau}\sigma T^4 = \frac{3}{4} F \left| \tau = \int_z^\infty \kappa\rho \, dz \right| \rightarrow \sigma T^4(\tau = 2/3) = F \tag{2.40}$$

τ represents the optical depth at geometrical depth z, F the energy flux through the atmosphere. We have made a second assumption, that there is no incident flux from outside the atmosphere. If the assumption of ν being constant with height still holds true and the heat is generated near the midplane, F is then approximately constant with height as well and equal to $\sigma T_\mathrm{s}^4(r)$. One than finds $\sigma_\mathrm{SB} T^4 = 3/4(\tau + (2/3))F$. We get further with κ constant with z that $\tau = \kappa\Sigma/2$ and using 2.35 the temperature at the midplane:

[10] The Eddington approximation is a special case of the two stream approximation for radiative transfer, in which the radiation propagates only in two discrete directions. It is used to obtain spectral radiance in a „plane-parallel"medium. In such a „plane-parallel"medium the properties only vary in the perpendicular direction. The two components (directions) of the radiation field are one component outward and a component inward.

$$T^4 = \frac{27}{64}\sigma^{-1}\Omega^2\nu\Sigma^2\kappa. \tag{2.41}$$

An equation for the disk's thickness can also be found by using the equation of state as well as 2.45:

$$\frac{H}{r} = \left(\frac{\mathcal{R}}{\mu}\right)^{2/5}\left(\frac{3}{64\pi^2\sigma}\right)^{1/10}\left(\frac{\kappa}{\alpha}\right)^{1/10}(GM)^{-7/20}r^{1/20}(f\dot{M})^{1/5} \tag{2.42}$$

$$\text{with} \qquad \left| r_6 = \frac{r}{10^6\text{cm}},\ \dot{M}_{16} = \frac{\dot{M}}{10^{16}\text{g/s}} \text{ and } f = 1 - \left(\frac{r_i}{r}\right)^{1/2} \right|$$

$$= 510^{-3}\alpha^{-1/10}r_6^{1/20}\left(\frac{M}{\dot{M}}\right)^{-7/20}(f\dot{M}_{16})^{1/5}.$$

One can see from this formula that it is very immune to changes of α, κ and r. Moreover, it should be kept in mind that 2.42 is derived under the assumption that energy dissipation takes place in the disk and not near the object's surface. If this would be the case, the internal temperature would be closer to the surface temperature of the central object.

2.4 Radiative Efficiency of Accretion Disks

The time scale for a disk to radiate away the energy released from the accreted gravitational potential energy is the accretion time scale:

$$\tau_{\text{acc}} \approx \frac{1}{\alpha\Omega_{\text{k}}}\left(\frac{r}{H}\right)^2. \tag{2.43}$$

As mentioned in the following section, in thin disks with $H/r \ll 1$ the accretion time scale is much longer as the thermal time scale τ_{therm}. Following these considerations there is sufficient time for local balance to exist between the viscous dissipation and radiative cooling, and the disk is rather cool. [11] Such radiatively inefficient disks are called „quasi-spherical“ and are named after the condition that those disks tend to be rather thick $H/r \sim O(1)$. Caution must be taken using this designation, as a spherical model would not be appropriate describing these disks. The „quasi-spherical“ flow has angular momentum and the inward movement of matter is governed by the rate at which angular momentum transport happens. The accretion time scale in such flows $\tau_{\text{acc}} \sim 1/(\alpha\Omega)$ is longer than the accretion time scale in spherical disks, $1/\Omega$. Further distinctions and specifications are made in the next sections. Finally it is also important that the radiative efficiency depends on the surface of the central object,i.e. whether it has a solid surface, which is the case considering neutron stars, planets or main sequence stars, or not (black holes). (Spruit 1996a)

[11] This holds true for the standard disk. Which does not mean that there are not accretion flows with the same order of accretion timescale that are radiatively inefficient.

2.5 Different Types of Disks

2.5.1 Geometrically Thin Disks

Steady Thin Disks

The discussion in this subsection is based on the work of G. Mamatsashvili 2011. Referring to the fact that changes in the radial structure of disks take place on long time scales $\tau_{\text{visc}} = r^2/\nu$, as described in 2.2, and that in many systems external conditions change on longer time scales than τ_{visc}, a stable disk can be described as a steady disk, i.e. $\partial/\partial t = 0$. Using this limitation for 2.11, we get:

$$r\Sigma v_{\text{r}} = \text{const.} \tag{2.44}$$

The mass flux towards the central mass is constant and equal to the accretion rate $\dot{M}$, see 2.46. The surface density distribution can be rewritten as

$$\nu\Sigma = \frac{1}{3\pi}\dot{M}\left[1 - \beta\left(\frac{r_{\text{i}}}{r}\right)^{1/2}\right], \tag{2.45}$$

$$\dot{M} = 2\pi r\Sigma(-v_{\text{r}}). \tag{2.46}$$

Here r_{i} represents the inner radius of the disk and β is a free parameter. Using 2.16 we get

$$Q(r) = \frac{3GM\dot{M}}{8\pi r^3}\left[1 - \left(\frac{r_{\text{i}}}{r}\right)^{1/2}\right]. \tag{2.47}$$

This equation of dissipated energy of a steady disk does not have an explicit dependence on ν, as we were able to use conservation laws to eliminate viscosity. It relies on the assumption that ν can adjust itself to give the required $\dot{M}$. Other disk properties (Σ, v_{r} etc.) do of course rely on ν.

Using 2.47 an equation for the disk's luminosity can be derived:

$$L(r_1, r_2) = 2\int_{r_1}^{r_2} Q(r) 2\pi r \, dr \tag{2.48}$$

$$L(r_1, r_2) = \frac{3GM\dot{M}}{2}\left[\frac{1}{r_1}\left(1 - \frac{2}{3}\left(\frac{r_*}{r_1}\right)^{1/2}\right) - \frac{1}{r_2}\left(1 - \frac{2}{3}\left(\frac{r_*}{r_2}\right)^{1/2}\right)\right] \tag{2.49}$$

$$= |r_1 = r_*, \; r_2 \to \infty| \, L_{\text{disc}} = \frac{GM\dot{M}}{2r_*} = \frac{1}{2}L_{\text{acc}} \tag{2.50}$$

Again r_* refers to the stellar radius. In conclusion, the total disk luminosity is half the luminosity gained through the accretion process. The remaining luminosity is emitted in the boundary layer of the disk.

Radiation Pressure Dominated Disks

The following considerations refer to the work of H.C. Spruit 1996a.
X-ray binaries (XRB) are a class of binary stars, where matter of one component, the so called donor, is falling onto the second object, mostly a very compact object, like a neutron star, a black hole or a white dwarf, called the accretor. These systems are luminous in X-rays, originating from the gravitational potential energy of the infalling matter. In the inner regions of disks around such XRB's it is possible for the radiation pressure to exceed the gas pressure. This, in turn, will lead to a different expression for the disk thickness. So the pressure (P_{tot}) must be written as a sum of both, the radiation pressure P_{r} and the gas pressure P_{g}:

$$P_{\mathrm{tot}} = P_{\mathrm{r}} + P_{\mathrm{g}} = \frac{1}{3} a T^4 + P_{\mathrm{g}} \tag{2.51}$$

Using 2.41 in combination with 2.47, for $P_{\mathrm{r}} \gg P_{\mathrm{g}}$, $\tau \gg 1$, $\Sigma = 2H\rho_0$ and $f = 1 - (r_{\mathrm{i}}/r)^{1/2}$ we get an approximation for the disk's thickness:

$$cH = \frac{3}{8\pi}\kappa f \dot{M} \left| \text{with } \frac{H}{r} = \frac{c}{\Omega r} \right| \rightarrow \frac{H}{r} \approx \frac{3}{8\pi}\frac{\kappa}{cr} f \dot{M} = \frac{3}{2} f \frac{\dot{M}}{\dot{M}_{\mathrm{E}}}. \tag{2.52}$$

Here r is the distance from the star and $\dot{M}_{\mathrm{E}}$ the Eddington accretion rate at this radius. We can derive from this formula that disks are not geometrically thin anymore near the star, if $\dot{M}$ is near the Eddington accretion rate $\dot{M}_{\mathrm{E}}$.

There are three local timescales in thin disks, two of them were already introduced. The dynamical timescale τ_{d}, which is the orbital time scale, and the radial drift time scale, which was defined as the viscous time scale τ_{visc}, see 2.15.

$$\tau_{\mathrm{d}} = \Omega^{-1} = \sqrt{\frac{r^3}{GM}} \tag{2.53}$$

$$\tau_{\mathrm{visc}} = \frac{r}{-v_{\mathrm{r}}} = \frac{2}{3}\frac{r^2 f}{\nu} \tag{2.54}$$

Using 2.45 and 2.46, we get $v_{\mathrm{r}} = -3\nu/2rf$, and further with $\nu = \alpha c_{\mathrm{s}}^2/\Omega$ and $c = H\Omega$ the viscous time scale is given as.

$$\tau_{\mathrm{visc}} = \frac{2}{3}\frac{f}{\alpha\Omega}\left(\frac{r}{H}\right)^2 \tag{2.55}$$

But we can also define a third time scale with respect to the disk temperature, the thermal time scale τ_{therm}. This time scale is found by equating the heating time scale τ_{h} with the cooling time scale τ_{c}. E_{t} is the enthalpy of the disk per unit of surface area [12] and $W_{\mathrm{visc}} = (9/4)\Omega^2\nu\Sigma$ the heating rate by viscous dissipation.

$$\tau_{\mathrm{h}} = \frac{E_{\mathrm{t}}}{W_{\mathrm{visc}}} \; and \; \tau_{\mathrm{c}} = \frac{E_{\mathrm{t}}}{2\sigma_{\mathrm{SB}} T_{\mathrm{s}}^4} \rightarrow \tau_{\mathrm{therm}} = \frac{1}{W_{\mathrm{visc}}} \int_{-\infty}^{\infty} \frac{\gamma P}{\gamma - 1}\, dz \tag{2.56}$$

$$\tau_{\mathrm{therm}} \approx \frac{1}{\alpha\Omega} \tag{2.57}$$

[12] For an ideal gas of constant ratio of specific heats γ.

For getting this approximation, numerical factors of order unity have been left out. One can see that 2.57 is of a factor $1/\alpha$ longer than the dynamical time scale and independent of most of the disk properties, which is in fact a result of the used α-parametrization. In most of the observed systems scientists have found that $\alpha < 1$ and therefore the three time scales can be ordered like this:

$$\tau_{\text{visc}} \gg \tau_{\text{therm}} > \tau_{\text{d}} \tag{2.58}$$

2.5.2 Beyond Thin Disks

Since in many astrophysical systems a large range of different length scales occur, they must be considered, as well as the different time scales. Finding an appropriate model that fits the observational data is mostly dependent on detailed numerical simulations in 2 or 3 dimensions. The thin disk equations are some good initial equations, with a lot of approximations, for finding models which are beyond these thin disks.

Radiation Supported-Radiatively Inefficient Accretion

The presented equations are based on the work of H.C. Spruit 1996a.
This type of accretion refers to a radiatively inefficient accretion, in which the radiation pressure dominates the flow. The gravitational energy release $W_{\text{grav}} \approx GM/(2r)$ is therefore converted into enthalpy of the gas and the radiation field. It is assumed that a fraction of the gravitational potential energy of ~ 0.5 stays in the flow as kinetic energy. As before, an ideal gas with constant ratio of specific heats γ and the radiation pressure, as defined in 2.51, are assumed.

$$W_{\text{grav}} = \frac{1}{2}\frac{GM}{r} = \frac{1}{\rho}\left[\frac{\gamma}{\gamma - 1}P_{\text{g}} + 4P_{\text{r}}\right]. \tag{2.59}$$

The virial temperature can be written as $T_{\text{vir}} = GM/(\mathcal{R}r)$ and assuming $\gamma = 5/3$ [13], equation 2.59 can be rewritten:

$$\frac{T}{T_{\text{vir}}} = \left[5 + 8\frac{P_{\text{r}}}{P_{\text{g}}}\right]^{-1}. \tag{2.60}$$

It is easy to see that for pressure dominated accretion $P_{\text{r}} \gg P_{\text{g}}$ the temperature is much less than the virial temperature. Assuming further hydrostatic equilibrium, the disk's thickness is given by

$$H \approx \left[(P_{\text{g}} + P_{\text{r}})]/\rho\right]^{1/2}/\Omega \tag{2.61}$$

or following 2.4 by $H/r = (T/T_{\text{vir}})^{1/2}$ and therefore $H/r \sim O(1)$. Consequently, in the limit of $P_{\text{r}} \gg P_{\text{g}}$, which means $T < T_{\text{vir}}$, the accretion flow is geometrically thick.

Trying to make statements with regard to the luminosity and the energy flux, one can start from 2.59, which yields, with $P_{\text{r}} \gg P_{\text{g}}$, to

$$\frac{GM}{2r} = \frac{4}{3}\frac{aT^4}{\rho}. \tag{2.62}$$

[13] Which means fully ionized monoatomic gas.

Following some approximations and equation 2.62, one gets the energy flux as an expression of the Eddington flux, $F_{\mathrm{E}} = L_{\mathrm{E}}/(4\pi r^2)$:

$$F = \frac{4}{3}\frac{\mathrm{d}}{\mathrm{d}\tau}\sigma T^4 \approx \frac{4}{3}\frac{\sigma T^4}{\tau}, \tag{2.63}$$

$$\text{with} \left| \tau = \int_z^\infty \kappa\rho \mathrm{dz} \to \tau = \kappa\Sigma/2 \ \text{ and } \ \Sigma \approx 2H\rho \ \text{ and } \ \sigma = \frac{ac}{4} \right|$$

$$F = \frac{1}{8}\frac{GM}{rH}\frac{c}{\kappa} \tag{2.64}$$

$$F_{\mathrm{E}} = \frac{c}{\kappa}\frac{GM}{r^2} \to F = F_{\mathrm{E}}\frac{r}{8H} \tag{2.65}$$

Taking into account that $H/r \approx 1$, one finds that the luminosity of a radiation pressure dominated, radiatively inefficient accretion flow is of the order of the Eddington luminosity. A dimensionless value for the accretion rate can be derived. The accretion rate is of the order of $\dot{M} \sim 3\pi\nu\Sigma$, where $\Sigma = \int \rho \mathrm{dz}$ is the surface mass density, and $\dot{M}_{\mathrm{E}} = RL_{\mathrm{E}}/(GM\eta) = 4\pi Rc/(\eta\kappa)$ represents the Eddington accretion rate onto the central object of size R.

$$\dot{m} = \frac{\dot{M}}{\dot{M}_{\mathrm{E}}} \approx \frac{\nu\rho\kappa}{c} \ . \tag{2.66}$$

The Eddington accretion rate differs due to the efficiency η, since the conversion of gravitational energy into radiation varies with the central object. (For instance a realistic value for the accretion onto a black hole is $\eta = 0.1$ or onto neutron stars $\eta \approx 0.4$, depending on the radius of the star.) A further assumptions that the viscosity scales with the gas pressure $\nu = \alpha P_{\mathrm{g}}/\rho\Omega_{\mathrm{k}}$ is made and with $2H/r \sim O(1)$ a mathematical solution for the disk's temperature can be found:

$$T^5 \approx \frac{(GM)^{3/2}}{r^{5/2}}\frac{\dot{m}c}{\alpha\kappa a\mathcal{R}}. \tag{2.67}$$

The temperature is low compared with the virial temperature in such flows and it should be mentioned that in the case of a dependence of the viscosity on the total pressure $P_{\mathrm{tot}} = P_{\mathrm{r}} + P_{\mathrm{g}}$, it would be even lower. In order to fulfill the radiation pressure and advection dominated aspect, the flow has to be optically thick.
As mentioned, different timescales have to be taken into account. In the following the cooling as well as the accretion time scale are noted:

$$\tau_{\mathrm{c}} = \frac{E}{F} \left| \text{with } E \approx aT^4H \text{ and } 2.63 \right| = 3\tau\frac{H}{c}. \tag{2.68}$$

E represents the energy density, vertically integrated at a distance r.

$$\tau_{\mathrm{acc}} = \frac{2\pi r^2\Sigma}{\dot{M}} \tag{2.69}$$

$$\frac{\tau_{\mathrm{c}}}{\tau_{\mathrm{acc}}} \approx \frac{\kappa}{\pi rc}\dot{M} = \frac{4}{\eta}\dot{m}\frac{R}{r} \ , \tag{2.70}$$

using $\tau = \kappa\Sigma/2$ and a factor of $(3/4)H/r \sim O(1)$ has been neglected. Consequently, accretion has to be of the order of the Eddington limit or above for such flows to be both advection and radiation dominated. This postulate can also be expressed in terms of a critical radius, the trapping radius $r_t/R \approx 4\dot{m}$. Inside this radius the disk is advection dominated, outside this radius the radiation field can not be strong enough to maintain a disk with $H/r \sim 1$. (Asmus 2008) Therefore the shape above the critical radius tends to be thin, which does not exclude the radiation pressure dominated condition, but the case of an advection dominated flow. These accretion flows, which accrete above the Eddington limit are called „radiation supported accretion tori“.

Advection Dominated Accretion Flows (ADAF)

Advection dominated accretion disks are disks in which gravitational energy is not completely locally released through radiation processes. The advective energy flux is taken into account in the energy budget, i.e. these disks represent radiatively inefficient flows and occur when the optical depth is either very small (Optical Thin Case) or very large (Optical Thick Case). A significant part of the energy is accreted with the matter by the central object. Moreover, these flows are susceptible to produce outflows and it is suggested that advection dominated accretion may provide an explanation for the slow spin rates of some accreting stars. As the gas rotates slower than the Keplerian velocity, the central star cease to spin up long before the break-up. These flows are named just after there definition, Advection Dominated Accretion Flows (ADAF). Two different scenarios are discussed:
1) The density of the gas, building up the accretion disk, is so thick that the photons on their way outside are, due to the frequent scattering, not fast enough and therefore trapped inside the disk, where they will move inward with the matter and fall onto the central object. (This kind of accretion flows are most likely to be present around black holes.) In this case it is expected that the radiation pressure at the inner part of the disk causes an expansion of the disk in vertical direction.
2) The second scenario illustrates the exact converse situation, where the density of the gas is extremely low. Considering this situation, it is no problem for the photons to escape the disk, but the interaction cross section is too low for efficient cooling, which means that the gas is going to heat up to very high temperatures, comparable with the solar corona. (Asmus 2008)
The mathematics of both scenarios predict very high radial velocities in the inner part of the disk. Therefore, a critical point, the sonic point, at which the matter flux goes into the supersonic state, is of special interest, see also 2.1.2. In a mathematical view the sonic point refers to the critical point r_{crit} where the denominator of the equation of motion vanishes. Following the work of Asmus 2008.

$$\frac{\mathrm{d}v_{\mathrm{r}}}{\mathrm{d}r} = \frac{1}{D}\left[r v_{\mathrm{r}}(\Omega^2 - \Omega_{\mathrm{k}}^2) - \frac{\gamma-1}{\gamma+1}\frac{1}{\rho}(q_+ + q_-) - \frac{2}{\gamma+1}c_{\mathrm{s}}^2 v_{\mathrm{r}}\left(\frac{1}{\Omega_{\mathrm{k}}}\frac{\mathrm{d}\Omega_{\mathrm{k}}}{\mathrm{d}r} - \frac{1}{r}\right)\right] = \frac{N_1}{D}. \tag{2.71}$$

Here γ is the ratio of the specific isobaric and isochore heat, c_{s} the speed of sound, v_{r} the radial velocity, Ω the angular velocity, ρ the density and q_+/q_- the viscous dissipation rate and radiative loss rate. This is the so-called singularity condition (SB from the German word „Singularitätsbedingung“). As the physical quantities have to be determined and finite, another condition must be taken into account, the regularity condition (REB from „Regularitätsbedingung“), that says that the nominator (N_1) at the critical point must vanish as well. (Asmus 2008)

The further discussion is based on the work of Spruit 1996a. Taking a look at the underlying mathematics, one finds that the density of the gas ρ, its radial velocity v_{r}, the angular velocity Ω and the speed of sound c_{s} satisfy four differential equations, the continuity equation, the radial and azimuthal components of the momentum equation and the energy equation:

$$2\pi r\Sigma v_{\mathrm{r}} = \dot{M} = \mathrm{const.}, \tag{2.72}$$

$$r\Sigma v_{\mathrm{r}}\partial_r(\Omega r^2) = \partial_r(\nu\Sigma r^3\partial_r\Omega), \tag{2.73}$$

$$v_\mathrm{r}\partial_r v_\mathrm{r} - (\Omega^2 - \Omega_\mathrm{k}^2)r = -\frac{1}{\rho}\partial_r p, \tag{2.74}$$

$$\Sigma v_\mathrm{r} T \partial_r S = q^+ - q^-, \tag{2.75}$$

using p as the total pressure in 2.74. In equation 2.75 the left hand side represents the advected entropy, T is the temperature and S the entropy. q^+ and q^- represent, as in 2.1.2, the height-integrated viscous dissipation rate and the radiative loss rate:

$$q^+ = \int Q_\mathrm{v}\mathrm{dz}\ , \qquad\qquad q^- = \int \mathrm{div}F_\mathrm{r}\mathrm{dz}. \tag{2.76}$$

Considering the case of a thin disk, equations 2.72 and 2.73 stay unchanged, whereas 2.74 simplifies to $\Omega^2 = \Omega_\mathrm{k}^2$ and 2.75 to $q^+ = q^-$. (Spruit 1996a) The difference between the energy input per unit area due to viscous dissipation and the energy loss through radiative cooling, which is the net energy advection rate, can be written differently (Narayan and Yi 1994):

$$q_\mathrm{adv} = q^+ - q^- = \frac{2\alpha\rho c_\mathrm{s}^2 R^2 H}{\Omega_\mathrm{k}}\left(\frac{d\Omega}{dR}\right)^2 - q^- \equiv f\frac{2\alpha\rho c_\mathrm{s}^2 R^2 H}{\Omega_\mathrm{k}}\left(\frac{d\Omega}{dR}\right)^2. \tag{2.77}$$

Here f measures the degree to which the flow is advection-dominated. Therefore, $f = 1$ represents the extreme limit where no radiative cooling is present and $f = 0$ the case of very efficient cooling. When radiative loss is neglected, i.e. $q^- = 0$, the characteristic properties are seen most clearly. If $\alpha = \mathrm{const}$, $q^- = 0$, and an ideal gas with constant ratio of specific heat γ is assumed, the entropy is given by (Spruit 1996a):

$$S = c_\mathrm{v}\ln\left(\frac{p}{\rho^\gamma}\right). \tag{2.78}$$

c_v refers to the specific isochore heat. Based on the considerations above equations 2.72 - 2.75 have no explicit length scale and a special, self-similar solution, in which all quantities are powers of r, exists. These quantities are summarized in the following:

$$\Omega \sim r^{-3/2}, \qquad\qquad \rho \sim r^{-3/2}, \tag{2.79}$$

$$H \sim r, \qquad\qquad T \sim r^{-1}. \tag{2.80}$$

The following self-similar solutions hold true for the limit $\alpha \ll 1$:

$$v_\mathrm{r} \approx -\alpha\Omega_\mathrm{k} r\left(9\frac{\gamma-1}{5-\gamma}\right), \tag{2.81}$$

$$\Omega \approx \Omega_\mathrm{k}\left(2\frac{5-3\gamma}{5-\gamma}\right)^{1/2}, \tag{2.82}$$

$$c_\mathrm{s}^2 \approx \Omega_\mathrm{k}^2 r^2 \frac{\gamma-1}{5-\gamma}, \tag{2.83}$$

$$\frac{H}{r} \approx \left(\frac{\gamma-1}{5-\gamma}\right)^{1/2}. \tag{2.84}$$

The precise form of these expressions depends on the way vertical integration is done. In 2.81 one can see that $v_r \sim \alpha$, i.e. the radial velocity is in principal determined by the efficiency of the viscosity moving angular momentum outwards. The radial speed tends to be much larger in advection dominated flows, since $\nu \sim \alpha c_s^2/\Omega_k$, than in thin disks. Taking a look at 2.82, one finds that in the case of $\gamma \to 5/3$ Ω goes to zero and the solution is the Bondi spherical accretion solution[14] for this γ. In 2.83 the speed of sound is comparable to the angular speed Ω_k, which means that the temperature of the accreted gas is almost virial. Which is plausible, as the gas has no way to cool. Moreover, when $c_s \sim \Omega_k$, H is comparable to R and the flow is quasi-spherical. (Spruit 1996a) The comparison with numerical solutions shows that the self-similar solution is valid in an intermediate regime $r_i \ll r \ll r_0$, and only exists if $1 < \gamma \leq 5/3$. For γ close to 1 the disk temperature and thickness vanish. For $\gamma \to 5/3$ the rotation rate vanishes, since in the case of spherical accretion no solution for $\gamma > 5/3$ exists. Steady advection dominated accretion can not have angular momentum in this case. As for a fully ionized gas $\gamma = 5/3$ the question arises how an adiabatic flow will behave in this case. Ogilvie 1999 described the asymptotic behavior of a viscously spreading disk analogous to the asymptotically accretion of mass to the central object, while all the angular momentum travels outward to infinity. For $\gamma = 5/3$ the rotation rate at a fixed r tends to zero. The size of the slowly rotating region expands as $r \sim t^{2/3}$ and the angular momentum is carried away from the inner regions almost completely. (Spruit 1996a) It is most likely that astrophysical systems have both, advection-dominated and standard cooling zones at different radii. The gas in ADAF's is capable of spontaneously escaping to infinity, which may generate an explanation for outflows, such as jets.(Narayan and Yi 1994)

It should be mentioned that there are other important flows occurring in astrophysical systems, such as the optically thin radiatively inefficient flows (ISAFs) which are mentioned in the following chapter, since they are related to accretion onto black holes. (Spruit 1996a) In figure 2.2 different branches for advection dominated and thin disks in dependence on the accretion rate and the optical depth of the flow are shown for different α. The Ion Supported Accretion Flows (ISAF) are discussed later in 4.3.3.

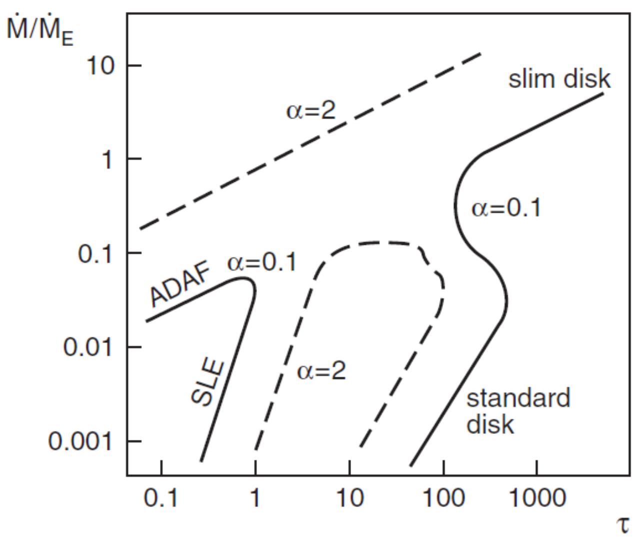

Figure 2.2: Branches of advection dominated flows and thin disks dependent on the accretion rate $\dot{m} = \dot{M}/\dot{M}_E$ and the optical depth of the flow τ for different values of α.
Optically thin branches: ISAF and SLE (Shapiro-Lightman-Eardly).
Optically thick branches: Slim disk (radiation dominated disk) and SS (Shakura and Sunyaev standard disk).
Advection-dominated: ISAF and the Slim disk.
Geometrically thin: SLE and SS. [15] (Spruit 1996a, p. 37)

[14] Bondi-Hoyle Accretion: We are considering the case of a star with mass M accreting spherically symmetrical from a large gas cloud, which is an approximation of the real situation of an isolated star in the interstellar medium. The magnetic field strength, the bulk motion and the angular momentum of the interstellar gas can be neglected with respect to the star. This case was first considered by Hoyle and Lyttleton (1939) and later by Bondi and Hoyle (1944). The case when the star is at rest, i.e. the accretion of the gas is in relative motion with respect to the star, was first studied by Bondi (1952) and this case of accretion is therefore named after him. (Juhan Frank and Raine 2002)

[15] In both cases, in an ADAF (Advection Dominated Accretion Flow) as well as in an ISAF (Ion Supported Accretion Flow) the radiation process is sufficiently weak. The differences are that ISAFs form a two-temperature plasma and an advection dominated accretion flow is possible for a very large or a very small optical depth. In Figure 2.2 the same value of α, for both types of flows, is assumed, labeled with „ADAF“.

2.6 Non-Gravitational Instabilities of Disks

The following discussion is based on the work of Spruit 1996a. In many disks something like outbursts, transients or an episodic behavior of the accretion can be observed. This irregularities occur due to some instabilities in the disk. Many models have been predicted explaining such phenomena. The most developed models are those, that are based on a temperature dependence of the viscous stress for instabilities. For comparison with the previous sections, the α-parameter will be a function of H/r. If this is a sufficiently increasing function, α is large in hot states and low in cool states, which will cause a runaway effect: starting at the stationary state at the mean accretion rate and considering a temperature increase, α goes up. Consequently, the viscous stress increases, which, in turn, increases the mass flux $\dot{M}$. An increase in mass flux once again increases disks temperature and this runaway will result in a hot state. Following this considerations we conclude, that if the mass flux is larger than average, the disk empties partly, which reduces the surface density and the central temperature. Therefore, a cooling front occurs which brings the disk to a cool state, with an accretion rate below the mean. This mechanism shows a switch back and forth between a hot and cool state of disks. It also predicts outbursts that reasonably well describe the observational data of soft transients.
Another reasonable possibility is the dynamical instability of the outer edge of a disk. This causes an oscillation that grows into a strong excentric perturbation. This has been confirmed with 2D numerical simulations. This instability will cause shock waves, spreading mass over most of the Roche lobe and simultaneously increasing the mass transfer onto the central object. This mechanism requires two-dimensional studies and does not depend on the viscosity.
Concluding, instabilities can occur due to many effects. Cooling rates can cause thermal instabilities. Or the instabilities may result from the dependence of viscosity on some disk properties.

2.6.1 Jet Formation in Disks

Jets, that are strongly collimated outflows, are seen in nature associated with Herbig-Haro objects, dying stars, micro quasars, quasars and radio galaxies. (Lynden-Bell 2002) Jets with relativistic flow speeds are especially known from stellar as well as from galactic black holes. (The case of accretion onto these will be discussed in chapter Accretion onto Black Holes.) Outflows with more modest velocities are observed in protostars, accreting neutron star (Cir X-1) and accreting white dwarfs (R Aqr). As their appearance emerge in many cases with the presence of an accretion disk, a connection between disks and jets is very likely. However, not all systems with accretion disks form jets, not all the time respectively. This leads to the question which mechanisms can produce such jets. (Spruit 1996a) The models for explaining the jet formation can be divided into three classes:

1) Hydrodynamic models, that can explain collimation by vortices around black holes or by self-similar thick disks.
2) Wind models with jets collimated by the local magnetic field of the rotating object.
3) Models that include a large-scale, pre-existing magnetic field.

The fact that all jets are associated with electromagnetic phenomena, accompanied with the acceleration of some particles to very high (relativistic) speeds support the concept that jets themselves are an electromagnetic phenomenon. (Lynden-Bell 2002) De facto the magnetic model, in which outflows are produced by magnetic fields of a rotating object, has become the standard for explaining the development of jets. Synchrotron radiation allows an indirect detection and the Zeeman effect in spectral lines of young stellar objects and protoplanetary nebulae allows a direct detection of the magnetic fields of the flows. Most of the magnetic interaction is suggested to take place in the inner regions of the flow. Unfortunately, the vast majority of the detection does not give any information on this region. In the following, I will give a short overview of the magneto-centrifugal acceleration model, based on the work of H.C. Spruit 2010,

that incorporates three distinct regions. This section only gives a brief insight in this standard model for jet formation and does not contain all suggested mechanisms and models in this field of science as this would be beyond the scope of this work. For more details see Lynden-Bell 2002, Spruit 1996b, Kato and S. Mineshige 2004 and Spruit 2010.
The three distinct regions, that play different roles in the formation of the jet, are (Figure 2.3) the

1) **Launching region**
The kinetic energy of rotation dominates over the magnetic energy in the accretion disk. The field lines are 'anchored' in the flow and co-rotate with it. There is a transition from the high β-interior[16] to the magnetically dominated atmosphere of the disk. In this transition region the amount of matter flowing into the jet is determined. The mass flow rate being dependent on the surface temperature is mostly treated as an additional parameter, as the calculations are not detailed enough to model the physical conditions near the surface of the disk.

2) **Acceleration region**
Considering a cool disk, the atmosphere of the flow has low density and gas pressure. In the region extending above and below the disk the magnetic pressure dominates over the gas pressure and the field must be approximately force free $[(\nabla \times B) \times B] = 0$. The magnetic field forces the flow of gas into a co-rotation with respect to the disk. This flow experiences a centrifugal force which accelerates it along the field lines, depending on the inclination of the field lines. The centrifugal process does not work for field lines parallel to the rotation axis of the disk. The flow velocity increases almost linearly with distance from the rotation axis.

3) **Collimation region**
In the Alfvén Region the flow speed equals the Alfvén speed and has reached a significant fraction of its terminal value. As the flow accelerates in Region 2) the field strength decreases with distance from the disk. The magnetic field lines start limping behind which in turn causes a 'wound up' into a spiral. Beyond the Alfvén radius the flow continues to expand away from the axis, so the rotation rate of the flow gradually vanishes by the tendency to conserve angular momentum. If nothing else were happening, the field would be almost purely azimuthal as is shown in Figure 2.4. However, this state is not suggested to survive long for much beyond the Alfvén radius. The high degree of collimation, which is observed in many jets from different objects must be due to an additional effect beyond the Alfvén radius. [17]

Therefore, the gravitational energy is transferred into kinetic energy of rotation and afterwards into kinetic energy of the outflow via the magnetic field, powering the jet. These jets that are powered by the rotation of the object are, in the case of a black hole, suggested to consist of electron-positron pair plasma and in the case of a rotating disk of a normal electron-ion plasma. As those are not exclusive, it is quiet likely that the jet of a black hole is partly fed with mass from the disk, rather than with electron-positron pair plasma. Unfortunately, the transition between disk and outflow is the least understood in the theory of accelerated jets. There remain still open questions in explaining the whole phenomena, such as the nature and origin of strong and preferably highly ordered magnetic fields. In Figure 2.5 an image taken with the Hubble space telescope is presented. It shows a jet of a young star. (Spruit 2010)

[16] The plasma β represents the ratio of the plasma pressure to the magnetic pressure. When $\beta > 1$, then the gas pressure dominates over the magnetic pressure. [17] Collimation is used in the same sense as in optics, it measures the degree to which the field lines in the jet are parallel.

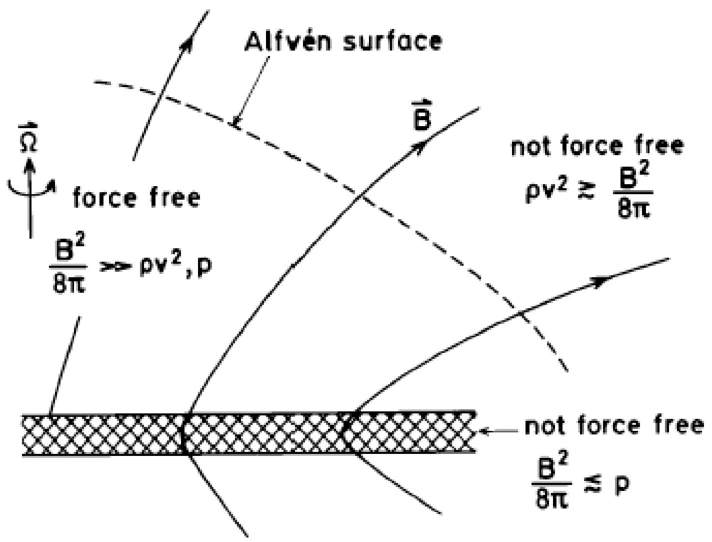

Figure 2.3: Different regions of the magneto-centrifugal acceleration model: The central object is located at the left side of the sketch. In the atmosphere up to the Alfvén structure the magnetic field dominates over the gas pressure. In this region the centrifugal acceleration takes place. (Spruit 2010, p. 2)

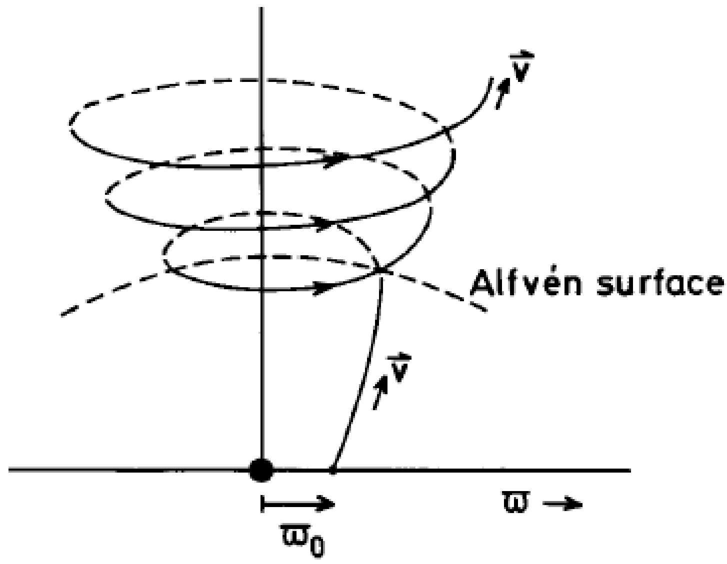

Figure 2.4: Field lines beyond the Alfvén radius: The field lines are lamping behind the rotation of their footpoints and begin to spiral up. The Alfvén surface itself is more complicated than this shematic illustration. (Spruit 2010, p. 3)

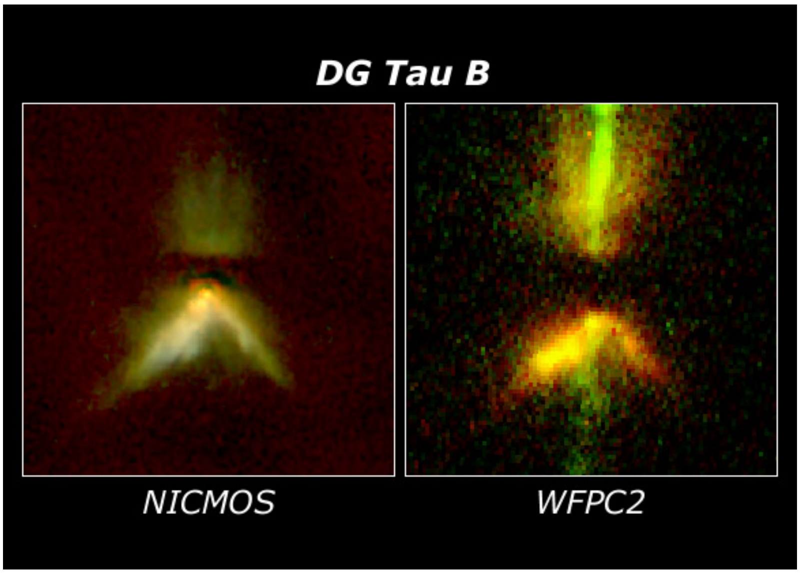

Figure 2.5: DG Tau B: An infrared NICMOS image and a visual Wide Field and Planetary Camera 2 (WFPC2) image, both taken with the Hubble space telescope. The thick black bar is a 500 AU dust lane, that indicates the presence of a disk surrounding the star. WFPC2 highlights the emerging jet and the central object, the bright red spot. It is located at the corner of the V-shaped nebula. (D. Padgett (IPAC/Caltech), W. Brandner (IPAC), K. Stapelfeldt (JPL),Chris Burrows (STScI))

3 Disk Models

3.1 The Boundary Layer Model

The first model of accretion disks has been proposed by Lynden-Bell and Pringle (Lynden-Bell and Pringle 1974). With regard to their paper, the dissipation of the converted gravitational energy leads to emission from a viscous Keplerian disk. This shining occurs first due to the radiation for a specific temperature, varying with the distance from the central mass, and second due to a boundary layer. Consequently, this model is called the „Boundary Layer model". (Alecian 2013) The boundary layer adresses the region of the flow which connects the accretion disk with the accreting central star. Considering a disk where the angular velocity Ω remains very close to the Keplerian one Ω_{K}, close to the boundary layer of radial extent b the angular velocity of the accretion material drops very rapidly from a near Keplerian value to the surface angular velocity of the star at that radius. Ω has therefore the form of the function shown in Figure 3.1. (Juhan Frank and Raine 2002) In this region up to half of the accretion luminosity may be released, which, in turn, leads to high temperatures. Here the largest flow velocities occur, which may be responsible for generating shocks and instabilities. A transition of the accretion material from centrifugal support, that dominates in the disk, to a pressure support, which dominates in the star, takes place. The boundary layer affects the structure of the disk as a whole. For gaining some insight into the complex radiative transfer, by which luminosity reaches the surface, radial and vertical fluxes need to be considered. In this narrow boundary layer turbulent viscosity plays a key role with respect to the dynamical and energetic evolution. (Narayan and Popham 1994)

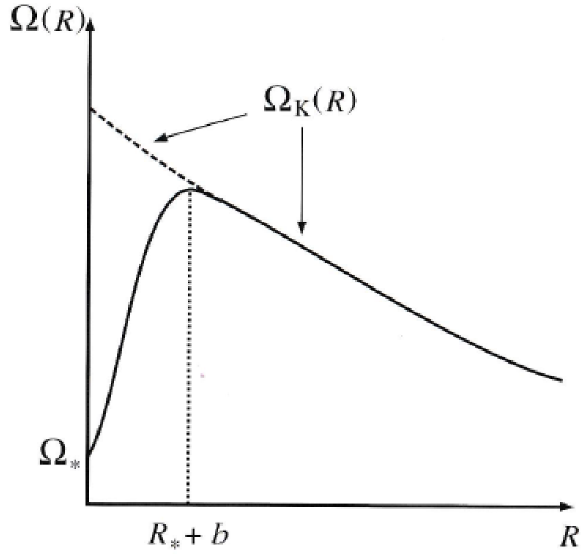

Figure 3.1: Distribution of the angular velocity Ω near the inner region of an accretion disk, with a decrease at the boundary layer at $r_* + b$ to the surface angular velocity of the star Ω_*. The boundary layer refers to the region $r_* \lesssim R \lesssim r_* + b$ (Juhan Frank and Raine 2002, p. 153). R_* means the stellar radius r_*, therefore $R_* = r_*$.

The boundary layer size is found to be:

$$b \sim \frac{r_+^2}{GM} c_{\mathrm{s}}^2 \sim \frac{H^2}{r_*} \tag{3.1}$$

This justifies the assumption that $b \ll r_*$, for $b \sim H^2/r_* \ll H \ll r_*$. (Juhan Frank and Raine 2002) A schematic picture of the boundary layer model is shown in Figure 3.1. The problem is reduced to that of a two-dimensional fluid, which is assumed to be polytropic. The simplified hydrodynamical equations describing such an accretion disk are given below.
In steady state the mass accretion rate is (see Steady Thin Disks)

$$\dot{M} = -2\pi r v_{\mathrm{r}} \Sigma = \mathrm{const.} \tag{3.2}$$

The steady state radial equation is given as

$$v_{\mathrm{r}} \frac{\mathrm{d}v_{\mathrm{r}}}{\mathrm{d}r} = \left(\Omega^2 - \Omega_{\mathrm{K}}^2\right) r - \frac{1}{\Sigma}\frac{\mathrm{d}P}{\mathrm{d}r}. \tag{3.3}$$

The flux of the angular momentum, where r_* is the equatorial radius of the star and ν the kinematic shear viscosity parameter, is

$$\dot{J} = \dot{M}\Omega r^2 + 2\pi r^3 \nu \Sigma \frac{\mathrm{d}\Omega}{\mathrm{d}r} \equiv j \dot{M} \Omega_{\mathrm{K}}(r_*) r_*^2. \tag{3.4}$$

$\dot{M}\Omega r^2$ describes the advection of angular momentum by the accreting material, and the second term represents the angular momentum flow associated with the viscous shear stress. For the identity a dimensionless parameter j has been introduced expressing $\dot{J}$ in terms of the characteristic flux of the angular momentum. In the classical theory of accretion disks it is assumed that $j = 1$. This means that the central star accretes angular momentum per unit mass equal to the specific angular momentum of a Keplerian orbit at the equatorial stellar radius. Furthermore, a description of ν is of great importance as it effects the nature of the flow in the boundary layer. Using the α-prescription would lead to supersonic radial infall, if α is larger than H/r_*, and may violate causality. For more detailed information please see Narayan and Popham 1994. They suggested that in the boundary layer region the eddy scale of the turbulent viscosity may be limited rather by the radial pressure scale height, $H_{\mathrm{p}} \equiv P/|\mathrm{dP}/\mathrm{dr}|$. Therefore, a modified prescription for ν has been proposed:

$$\nu = \alpha c_{\mathrm{s}} \left(\frac{1}{H^2} + \frac{1}{H_{\mathrm{p}}^2}\right)^{-1/2} \left(1 - \frac{v_{\mathrm{r}}^2}{v_{\mathrm{t}}^2}\right)^2. \tag{3.5}$$

Viscosity is produced by the transport of (angular) momentum by particles, which means that in reality shear stress can only propagate as fast as the particle velocities. With this prescription, in which v_{t} represents the maximum speed of the viscous particles, ν vanishes as the radial velocity approaches this critical propagation speed. This holds only for steady state flows. Boundary layer solutions described by this ν show that v_{r} never exceeds v_{t}. Between the star and the disk viscous contact is always maintained and there is no causality paradox. However, this parametrization is unlikely to be valid in detail under less restrictive conditions. (Narayan and Popham 1994) Straightforward, the net luminosity L_{tot} of the accretion disk L_{disk} and the boundary layer L_{BL} is

$$L_{\mathrm{tot}} = L_{\mathrm{disk}} + L_{\mathrm{BL}} = \frac{G\dot{M}M_*}{r_*}\left[1 - j\frac{\Omega_*}{\Omega_{\mathrm{K}}(r_*)} + \frac{1}{2}\frac{\Omega_*^2}{\Omega_{\mathrm{K}}^2(r_*)}\right]. \tag{3.6}$$

In the slow rotating regime we have $j \simeq 1$ and the luminosities can be written like

$$L_{\mathrm{disk}} = \frac{G\dot{M}M_*}{2r_*}, \qquad L_{\mathrm{BL}} = \frac{G\dot{M}M_*}{2r_*}\left[1 - \frac{\Omega_*}{\Omega_{\mathrm{K}}(r_*)}\right]^2. \tag{3.7}$$

3.6 and 3.7 were determined under the assumption that the total binding energy, released in the accretion, is bigger than the entropy carried into the star by the accreted material. The boundary layer will be optically thick and radiate roughly as a blackbody of area $\sim 2\pi r_* H \times 2$, if the accretion rate, and therefore the density in this region, is high enough. Moreover, we know the luminosity emitted by this area, 3.7. Therefore a characteristic boundary layer blackbody temperature is given by

$$4\pi r_* H \sigma_{\mathrm{SB}} T_{\mathrm{BL}}^4 \sim \frac{GM\dot{M}}{2r_*} \rightarrow T_{\mathrm{BL}} \sim \left(\frac{r_*}{H}\right)^{1/4} T_* \, . \tag{3.8}$$

A comparison with the characteristic blackbody temperature of the star T_*, see 2.36, yields to the right side of the expression. (Juhan Frank and Raine 2002)

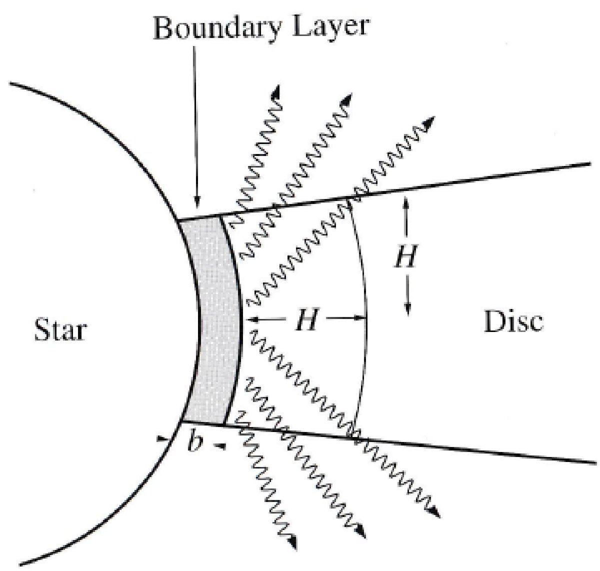

Figure 3.2: Shematic illustration of an optically thick boundary layer. Radiation emitted by the boundary layer emerges through a region of radial extent $\sim H$.
(Here H represents the half thickness of the disk.) (Juhan Frank and Raine 2002, p. 153)

3.2 The Flaring Disk

Since the observationally found spectral indices are higher than 4/3 there must be an additional source to the viscous accretion or to the light reprocessing. The suggested model is the one of a flaring disk. Regarding to this model the disk flares slightly with increasing radial distance.
The balance between the gravitational force of the central star (or astrophysical object) and the gas pressure gradient is known as the hydrostatic equilibrium. This pressure of the gas, at a radius r from the center and at distance z perpendicular to the midplane of the disk, is determined as

$$\frac{\mathrm{dP}}{P} = \frac{\Omega_K^2}{c_s^2} z \, \mathrm{dz}. \tag{3.9}$$

Ω_K refers here again to the Keplerian angular velocity and c_s to the speed of sound. As mentioned in 2.3 and 2.4 the scale height of the disk can be defined by

$$\frac{H}{r} = \left(\frac{c_s^2 r}{GM}\right)^{1/2} . \tag{3.10}$$

One can derive from this equation that, if the internal temperature of the disk ($T \propto c_s^2$) falls off more slowly than r^{-1}, the disk inflates with increasing distance. Due to the increasing thickness of the disk, the disk's surface is concave, which is illustrated in Figure 3.3.

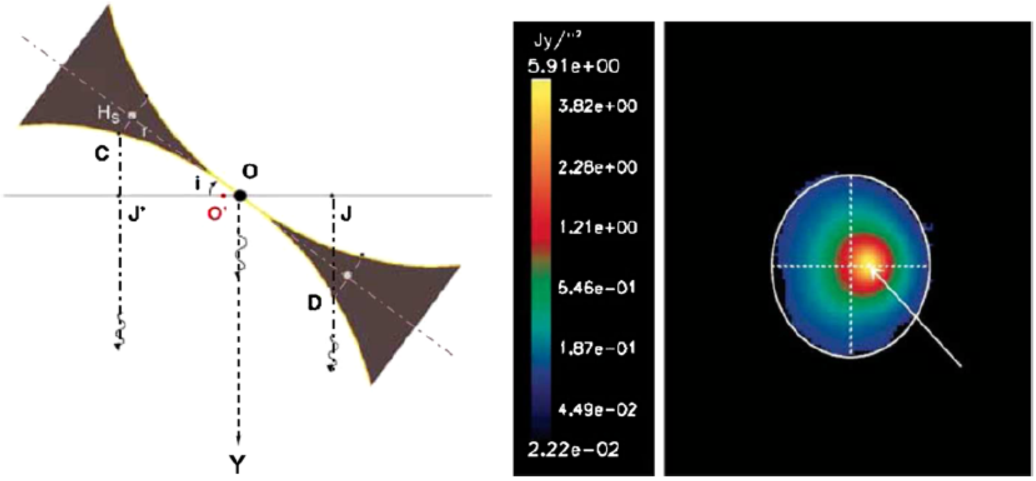

Figure 3.3: Illustration of a flaring disk
Left sketch: A schematic illustration of the flared disk of HD 97048 is shown. C and D are two points at the surface of the disk with same distances from the star, located in O. i defines the inclination between the line of sight and the disk axis. The disk is seen from below. For an observer the center of the disk is expected to be in O', due to the geometrical effect. *Right sketch*: The corresponding IR observation of HD 97048. As proposed in the left panel, the photo center, that is indicated with the white arrow, does not coincide with the geometrical center. (Alecian 2013, p. 190)

This flaring structure is supported by the gas and weakened by the dust, existing in the disk, as dust absorbs and reemitts the radiation and thus cools the disc. In the case of a vertically isothermal disk the surface temperature is equal to the interior temperature and so the scale height is proportional to $r^{1/8}$. Considering this value of the scale height the model of a flared disk seems to be plausible. In the case of an optically thick disk the flared disk will intercept more radiation than in the case of a completely flat disk. The descriptions in this paragraph refer to the work of Kenyon and Hartmann 1987, mentioned in Alecian 2013.

3.3 The Two-Layer Model

It is argued, that the cooling by the dust is overestimated by Kenyon and Hartmann 1987 due to the dust settling [18] within the disk. The more advanced two layer model refers to a steady, viscous, geometrically thin, optically thick flared accretion disk. The disk's dust and gas structure are shown in Figure 3.4. The disk structure is proposed as a combination of an optically thick viscous disk, in the mid-layer, and an optically thin (at IR wavelength) non-viscous atmosphere in the radial equilibrium, the two outer layers. According to this model the internal energy of the disk has two sources, the irradiation from the central star and the accretion.(Alecian 2013) In the mid-layer the dust and gas are in thermal equilibrium at the same temperature $T_\mathrm{g} = T_\mathrm{d} = T_\mathrm{mid}$. (Kraus 2003) The disk cools through thermal emission of the dust grains at infrared wavelengths, which leads to the observable infrared dust continuum radiation. (C.P. Dullemond and D'Alessio 2006) The atmosphere absorbs and/or scatters the stellar flux of the star. Consequently, the heating from the viscous interior as well as the stellar radiation absorbed determine the temperature of the atmosphere. (Alecian 2013) Therefore the temperature of the disk is determined

[18] Dust grains grow and the larger particles tend to settle to the mid-plane.

by a balance between cooling and heating. (C.P. Dullemond and D'Alessio 2006)
It has been found that the irradiated disk dominates the flux at wavelengths bigger than $1\mu m$. The spectral signature of some elements is strongly dependent on the accretion rate and stellar effective temperature.[19] As the accretion rate affects the viscous energy damped into the atmosphere and the stellar effective temperature the amount of radiative heating, it is proposed that observations can give an indication of the accretion rate of the central object. Consequently, such accretion features can be visualized in an emission spectrum the lower the accretion rate and the higher the stellar temperature, and in an absorption spectrum the lower the stellar temperature and the higher the accretion rate. (Alecian 2013)
Moreover, if the temperature structure is known the spectral energy distribution (SED) can be computed. The observable emission comes from three different wavelength regimes, illustrated in Figure 3.5:

a) A wavelength range depending on the minimum and maximum temperature of the dust inside the disk. This is the „energetic domain“of the SED as the main portion of energy is emitted here. In this domain the geometry of the disk is best reflected.

b) At longer wavelengths the SED turns over in a „Rayleigh-Jeans domain“. Here the slope depends on dust grain properties and the optical depth. The sub mm and mm fluxes reflect the disks mass.

c) A shorter wavelength range, which refers to the „Wien domain“of the disk's emissions. Here the stellar radiation contributes also to the SED and starts to dominate at near-infrared or optical wavelengths. (C.P. Dullemond and D'Alessio 2006)

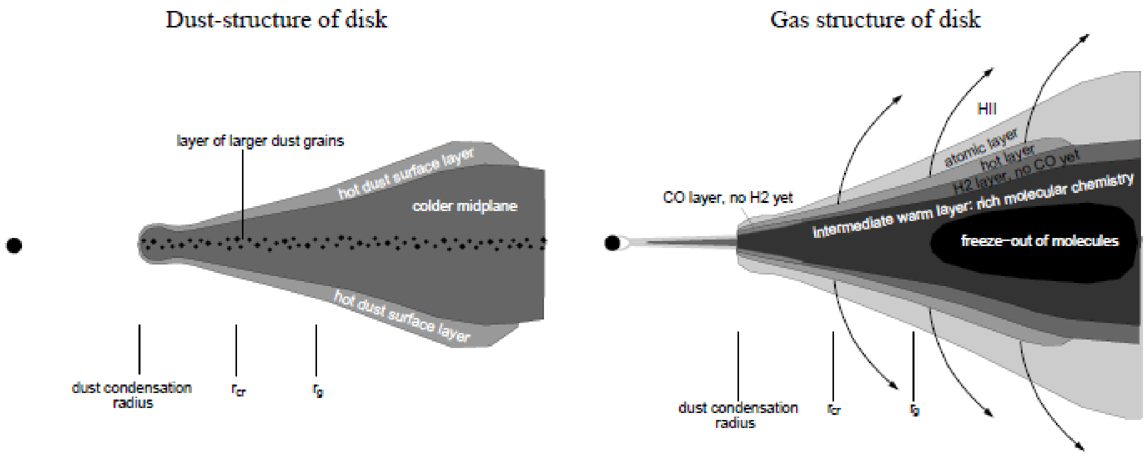

Figure 3.4: Schematic illustration of the gas and dust structure of a flaring protoplanetary disk. (C.P. Dullemond and D'Alessio 2006)

[19] The electronic, vibrational and rotational transitions of molecular and atomic elements is assumed to be the main source of opacity in the near- and mid-IR.

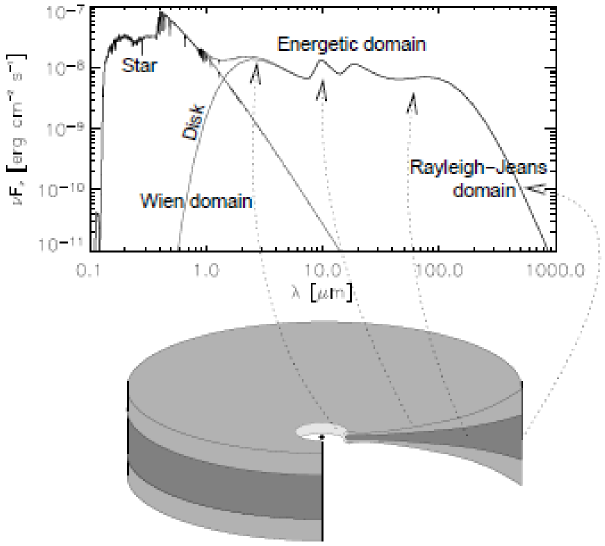

Figure 3.5: SED of a flared protoplanetary disk. The near-infrared and mid-infrared emission comes from small radii, the far-infrared emission comes from the outer regions and the (sub)millimeter flux from the midplane of the outer disk. Due to the inner rim there is a near-infrared bump. The infrared dust features originate in the warm suface layer and the underlying continuum is emitted by deeper (cooler) disk regions. (C.P. Dullemond and D'Alessio 2006, p. 4)

3.4 The Shakura-Sunyaev Disk

The discussion in this section is based on the book of Juhan Frank and Raine 2002.
The Shakura-Sunyaev disk describes, as mostly mentioned in the literature, the standard or classical model of a steady α accretion disks. It delineates geometrically thin $H \ll r$, optically thick accretion disks. The disk's rotation velocity is equal to the Keplerian one ($\Omega = \Omega_K$). Further it is proposed that all the gained energy is radiated away. There is no advected energy, which simplifies the energy balance to $q^-_{thick} + q^+_{vis} = 0$. Additionally, the radial velocity is much lower than the rotation velocity ($v_r \ll \Omega$). Angular momentum is transported via some kind of turbulence and the solutions are based on the α viscosity prescription.

In the following the characteristic equations specifying the properties of this model are noted, based on the work of Asmus 2008. For the radial velocity one finds:

$$v_{\mathrm{r}} = \frac{\dot{J} v_{\mathrm{r,std}}}{\dot{M} r^2 \Omega_{\mathrm{K}}} + \frac{\nu}{\Omega_{\mathrm{K}}} \frac{\mathrm{d}\Omega_{\mathrm{K}}}{\mathrm{d}r}. \tag{3.11}$$

Here $\dot{J} = \dot{M} r^2 \Omega - \mathbf{T}$ is the angular momentum flux onto the central object per unit of time, with $\mathbf{T} = 4\pi r H \rho \nu r^2 \; \mathrm{d}\Omega/\mathrm{d}r$ referring to the torque. To avoid misunderstandings, below T is again used, as usual, for the temperature. (Asmus 2008) With the above mentioned definitions and with 2.4 (speed of sound) and 2.17 (viscosity) one finds:

$$\Omega_{\mathrm{std}} = \Omega_{\mathrm{K}}, \tag{3.12}$$

$$c_{\mathrm{s,std}} = \frac{\mathcal{R}T}{\mu} + \frac{aT^4}{3\rho}, \tag{3.13}$$

$$q^-_{\mathrm{thick}} = q^+_{\mathrm{visc}}, \tag{3.14}$$

$$\nu = \frac{\alpha c^2_{\mathrm{s,std}}}{\Omega_K}. \tag{3.15}$$

The equations for Σ, H, ρ etc. are expressed in terms of $R_{10} = R/(10^{10}\mathrm{cm})$, $m = M/M_\odot$ and $\dot{M}_{16} = \dot{M}/(10^{16}\ \mathrm{g\ s^{-1}})$, with $f = [1-(R_*/R)^{1/2}]^{1/4}$ and using M as the central object's mass, $\dot{M}$ the accretion rate and R the disk's radius, to get an idea of the typical sizes of the disk quantities. These are based on the book of Juhan Frank and Raine 2002.

$$
\begin{aligned}
\Sigma &= 5.2\alpha^{-4/5}\dot{M}_{16}^{7/10}m^{1/4}R_{10}^{-3/4}f^{14/5}\ \mathrm{g\ cm^{-2}}\\
H &= 1.7\cdot 10^{8}\alpha^{-1/10}\dot{M}_{16}^{3/20}m^{-3/8}R_{10}^{9/8}f^{3/5}\ \mathrm{cm}\\
\rho &= 3.1\cdot 10^{-8}\alpha^{-7/10}\dot{M}_{16}^{11/20}m^{5/8}R_{10}^{-15/8}f^{11/5}\ \mathrm{g\ cm^{-3}}\\
T_c &= 1.4\cdot 10^{4}\alpha^{-1/5}\dot{M}_{16}^{3/10}m^{1/4}R_{10}^{-3/4}f^{6/5}\ \mathrm{K}\\
\tau &= 190\alpha^{-4/5}\dot{M}_{16}^{1/5}f^{4/5}\\
\nu &= 1.8\cdot 10^{14}\alpha^{4/5}\dot{M}_{16}^{3/10}m^{-1/4}R_{10}^{3/4}f^{6/5}\ \mathrm{cm^2\ s^{-1}}\\
v_\mathrm{r} &= 2.7\cdot 10^{4}\alpha^{4/5}\dot{M}_{16}^{3/10}m^{-1/4}R_{10}^{-1/4}f^{-14/5}\ \mathrm{cm\ s^{-1}}
\end{aligned}
\tag{3.16}
$$

All mentioned quantities are not very sensitive to the actual value of α, since it does not enter any expression with a high power. This means, however, that the typical size of α cannot be discovered by direct comparison of a steady state disk theory with observations. Moreover, one sees that the radial drift velocity v_r is highly subsonic, whereas the Kepler velocity v_k is very supersonic. As mentioned above we see from equation 3.16 that the disk's opacity τ is high and therefore the disk is optically thick for any reasonable accretion rate. Last but not least the temperature at the midplane T_c and the surface temperature of the disk $T_\mathrm{s}(r)$ differ by a factor of 3.7, which suggests the disk to be roughly uniform in the vertical direction. The disk can extend to very large radii of the order of the Roche lobe of the accreting star, as long as the above noted relations remain valid. Unless α is very small, the disk's mass is small compared to that of the accreting star. In general α can be a function of $\dot{M}$, M, R and z, see Angular Momentum Transport/ Viscosity. The z-dependence can be ignored, if we interpret the α appearing in 3.16 as a vertically averaged α, because the disk equations treat the vertical structure as uniform (for example $T_\mathrm{c}(R,z) \simeq T_\mathrm{c}(R)$). The equations in 3.16 can be obtained without knowing the dependence of α on M, $\dot{M}$ and R. This, in turn, means that the above given solutions for Σ, H, ρ etc. are scarcely a solution at all in a strict mathematical sense. Since we do not know the dependence of α on M, $\dot{M}$ and R, the dependence of all the other disk quantities is unknown. Therefore, it is only possible to say how sensitive these equations are to our ignorance. It is important to say that, however, one gets consistent results for the disk quantities for $\alpha \lesssim 1$. But it should be kept in mind that the equations given in 3.16 cannot predict how disk properties change if M, $\dot{M}$ and R are varied. Moreover, there is a tendency for the importance of radiation pressure to gain relative to that of the gas pressure at smaller radii, which continues and intensifies in the region where electron scattering dominates the opacity. (Juhan Frank and Raine 2002) In the work of Shakura and Sunyaev 1973 the pressure gradient in radial direction is neglected and has no influence on the matter. Moreover, there is no transition to the supersonic region and therefore no critical point r_t can be found. This model simplifies many conditions but is more or less inconvenient describing accretion disks around black holes as the transition to the supersonic region is an important property of the inner region of the latter. (Asmus 2008)

4 Accretion onto Black Holes

Accretion flows are different for objects with solid surfaces, such as forming stars, forming planets, white dwarfs, neutron stars etc., and for those without, like black holes. It is important to distinguish between galactic, which means super massive black holes, and stellar black holes, which appear as single objects or in binary systems. Accretion onto black holes is of important interest. Supermassive black holes (SMBH) with masses $\sim 10^9 M_\odot$ are suggested to be the central objects in almost all massive galaxies, including our Milky way[20]. Those who are strongly accreting are called Active Galactic Nuclei (AGN). Although there is not much interaction with the SMBH in the Galactic Center the observational data support the theory of a weak accretion disk or some kind of matter orbiting the center. In the last section recent observational data of Saggitarius A* will be presented and discussed.
Research in the field of stellar black holes is important, to get deeper insight in the working mechanisms, of both types of black holes. The equations of the structure and the proposed mechanism of angular momentum transport introduced above for protoplanetary disks, still hold true for black holes but have to be slightly modified. Accretion onto black holes differs mainly because of the high accretion rate of the system due to the big mass of the object as well as on some details in the structure. For example in the case of accretion onto a compact object with a solid surface it is assumed that the disk (almost) reaches the stellar surface, which is most unlikely in the case of a black hole. The previously discussed mechanism of energy release, chapter 1 - 3, is the most effective one in accretion disks around black holes. Unfortunately, the central object cannot be directly observed and is veiled by the dust in the line of sight. Observing the surrounding accretion disk can give conclusions on the black hole's mass, some properties of it and the conditions in its environment. Further, it is very likely that most of the radiation is generated in the innermost region of the accretion disk, the inner rim of the disk. The location of this inner rim, as well as the specific role of accretion disks around black holes, their properties and their differences with respect to accretion disks around objects like forming stars and forming planets, neutron stars and white dwarfs, will be summarized in this chapter. The evolution of such a disk will be discussed for a stellar black hole in a binary system. The formation process of a disk around an SMBH will not be described in this thesis as much longer time and much higher mass scales have to be considered. The definition of the inner rim, the stable orbits around a black hole as well as the different types of accretion are certainly valid for both the stellar and galactic black holes.

For an elementary insight in black holes the work of Hawking 2001 and Thorne 1994 as well as for a compact introduction and overall view the work of Müller 2010 are suggested. Understanding this chapter requires basic knowledge on the physics underlying black holes.

4.1 Definition of the Inner Rim

Following classical considerations, for a test particle stable orbits around the central mass exist. The region at which stable orbits become no longer possible is called the marginal stable orbit region and is commonly described by the innermost stable circular orbit (ISCO) around the black hole. The question whether a particle falls onto the black hole or goes into a circular orbit depends mainly on the specific

[20] The supermassive black hole in the center of our Galaxy is quiescent and therefore per definition no AGN.

angular momentum, l, in the equation of the effective potential.

$$V_{\text{eff}}^2(r) = \left(1 - \frac{2GM_{BH}}{rc^2}\right)\left(1 + \frac{l^2}{c^2r^2}\right) \tag{4.1}$$

Using the speed of light c, r the distance from the black hole, M_{BH} the black hole's mass and G the universal gravitational constant. The stable orbits for test particles with different specific angular momenta are shown in Figure 4.1.

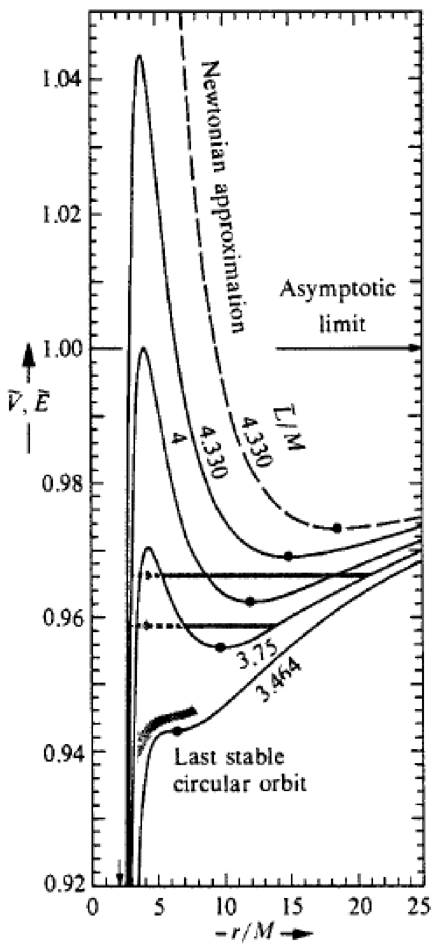

Figure 4.1: Effective potentials for test particles orbiting around a black hole with different specific angular momenta are shown in the Schwarzschild metric, a non rotating black hole. The minimal angular momentum is given with $l = 3.464$ and corresponds to the marginal stable orbit of the black hole. The thick horizontal lines represent the minimal energy that must be reached by the test particles to tunnel through the potential barrier in the case of microscopic black holes. (Asmus 2008, p. 5)

V_{eff} has a maximum at $l \geq 2\sqrt{3}GM_{BH}/c^2$ and there is no extremum if $l < 2\sqrt{3}GM_{BH}/c^2$. Consequently and as effects of the strong relativistic field, particles with $l > 0$ and $l < 2\sqrt{3}GM_{\text{BH}}/c^2$ fall into the gravitating mass. Particles with low (not just zero) angular momentum are captured by the hole. For a specific angular momentum $l = 2\sqrt{3}GM_{BH}/c^2$ the minimum corresponds to the innermost stable circular orbit. This ISCO, in turn is commonly associated with the inner rim of the accretion disk. As in nature accretion disks are not a composite of single test particles, but rather can be explained with a viscous flow, in which particles always lose energy, the definition of the inner rim must be modified. Due to this we will follow the description that the region in which the flow is decoupled from the viscous disk and falls in very short timescales onto the black hole is specified as the inner rim of the accretion disk. In this inner region of the accretion disk the self-gravitation of the gas does not play any role and the gravitation field is dominated by the mass of the Black hole. Therefore, this case is called Non-Self-Gravitating (NSG). (Asmus 2008)

4.2 Development of Accretion Disks Around Black Holes in Binary Systems

Stellar black holes are most likely to be found in binary systems. It is also quite likely that they are hidden among known optical objects, X-ray sources and the harder X-ray sources. (X-rays with photon energies above $5 - 10$keV are called hard X-rays.)

For explaining the development of an accretion disk around a black hole we consider the case of a binary system. In such a binary system we have a compact primary mass M_1 and a main sequence companion of mass M_2. Depending on the type of star, the matter outflow from the star's surface, which is referred to as the donor, varies from $2 \cdot 10^{-14}$, in the case of the Sun, up to $10^{-5} M_\odot$/year for the O-stars of the main sequence. In binary systems another additional strong matter outflow has to be beard in mind. This matter outflow is connected with the Roche limiting surface. If M_1 and M_2 orbit around each other with a separation a with orbital frequency

$$\Omega^2 = G(M_1 + M_2)/a^3, \tag{4.2}$$

the matter, suggested to be in a co-rotating frame and therefore stationary, experiences an effective potential. The Roche potential

$$\phi_R(\mathbf{r}) = -\frac{GM_1}{r_1} - \frac{GM_2}{r_2} - \frac{1}{2}\Omega^2 \mathbf{r}^2, \tag{4.3}$$

where $r_1 = |\mathbf{r} - \mathbf{r}_1|$ and $r_2 = |\mathbf{r} - \mathbf{r}_2|$ represent the distances of a point $\mathbf{r}$ to stars $1, 2$. Taking a closer look, one finds that the equipotential surfaces are unaffected by the other star near the central masses, at higher ϕ they are distorted and at a critical value the two parts of the surface touch. This two parts associated with the critical Roche potential ϕ_1 are called the Roche Lobe. (Spruit 1996a) If the Roche Lobe is filled, probably at the late stages of a star's life, when its radius starts to increase, there is strong matter outflow, mostly through the inner Lagrangian point. (See Figure4.2)

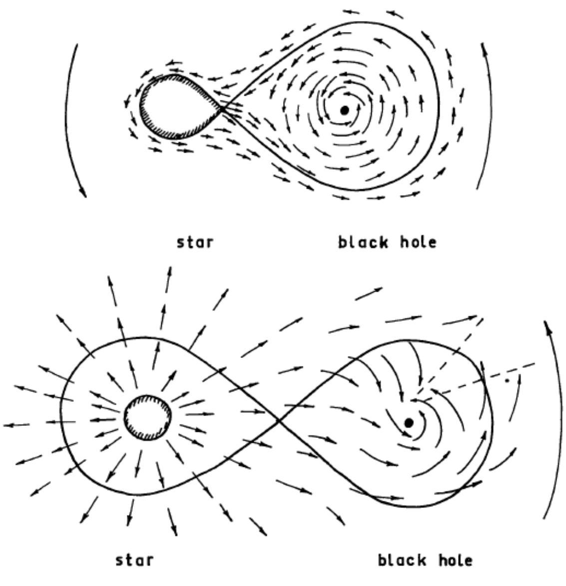

Figure 4.2: Roche-Lobe of a binary system
Upper Panel: The companion fills up its Roche Lobe and the outflow is mostly through the inner Lagrangian point.
Lower Panel: The outflow of the normal star, with a size much smaller than the Roche Lobe, is powered by a stellar wind. Gravitational capture of the matter by the black hole is probably caused by the kinetic energy loss of the matter in the shock wave. (Shakura and Sunyaev 1973, p. 338)

The force acting on the matter is not just given by equation 4.3. The gas cannot fall in radially on M_1 (the accretor), because the gas' orbit is influenced by the Coriolis force as soon as it moves and does not co-rotate anymore. A fraction of this matter outflow from one component is interacting with the gravitational field of the second component, the black hole. As discussed above, the matter has considerable angular momentum which prevents direct accretion. At some distance from the black hole the centrifugal force and the gravitational force are comparable and the matter starts to rotate in circular orbits. To approach the black hole mechanisms of angular momentum transport are necessary. Again the most probable mechanism is the formation of a disk around the black hole. During this accretion process, gravitational energy, as mentioned in former sections, is released. This energy in turn goes partly into kinetic energy of the disk and partly into the thermal energy of the disk. The latter is emitted by the disk. (Shakura and Sunyaev 1973)

4.2.1 Spectrum of the Disk

The following discussion is based on the work of Shakura and Sunyaev 1973. The observed spectrum of the radiation and the total energy release is mainly dependent on the mass flux $\dot{M}$ inwards. Moreover, the local radiation spectrum, which is formed in the upper layers of the disk, is dependent on the distance from the black hole, the density as well as on the matter and temperature distribution along the z-coordinate perpendicular to the disk's plane. The radiation can originate close to the radius where the forces of radiation pressure and gravitation are comparable. This radius in turn is dependent on the α-parameter. The smaller α the greater the effective radius of the radiating envelope and the lower the effective temperature of the radiation. As done above the α-parameter is assumed to be constant throughout the disk. As we will see later, the chosen value of α only plays a role considering the super-critical regime (page 42).
The luminosity of the black hole can be calculated using a slightly different equation than in the Introduction. $L = \eta_{\text{eff}}\dot{M}c^2$, where η_{eff} represents the efficiency of gravitational energy release. In the case of the Schwarzschild metric (non-rotating black holes) $\eta_{\text{eff}} \simeq 0.06$ and in the case of the Kerr metric (rotating black holes) η_{eff} can be up to 40%. Again we can assume the Eddington limit for accretion and luminosity, but there is no particular reason assuming an accretion equal to the critical value. In fact the optical luminosity of the black hole may be much higher. This luminosity arises from reemission of hard radiation of the hot central regions by the outer layers. For a better understanding one must bear in mind that the thickness of the disk increases with distance. If we follow the theory of disk accretion, one finds that the disk starts to thicken around $r > 150(\alpha m)^{2/21}\dot{m}^{16/21}$, which causes the real form of the disk, a saucer. As mentioned, the outer regions catch a significant part of the X-ray radiation of the inner regions. Due to the optical thickness of the disk, the surface absorbs and reemitts a certain part of the radiation, which leads to photoionization of the heavy elements. The radiation of softer photons causes a heating of the matter. This heating, accompanied by an outflow of the hot gas, increases the disk's thickness as well as the absorbed fraction of the hard radiation of the central regions. This reprocessed energy is visible in the spectrum as recombination radiation and resonance lines in the optical range. The luminosity as a function of the radius is shown in Figure 4.3.

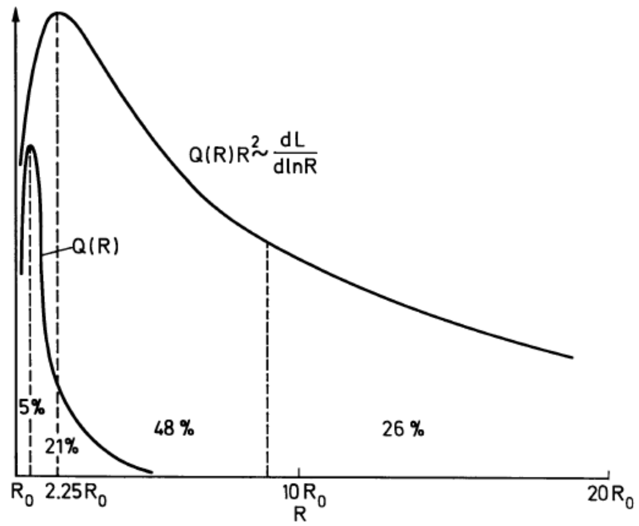

Figure 4.3: At a given radius R and with $\Delta R \sim R$ the function $Q(R)R^2$ ($Q(R)$ is the energy flux, radiated from the disk's surface) is proportional to the luminosity of the ring with a width ΔR. $R_0 = 3R_{\text{g}}$ represents the inner boundary of the disk, with R_{g} the gravitational or Schwarzschild radius. The numbers shown in the figure are the contributions of the corresponding regions to the integral luminosity. As we can see, most of the radiation is emitted near the inner rim of the accretion disk. (Shakura and Sunyaev 1973, p. 342)

There is the possibility of some unusual optical appearances or variabilities of the luminosity of the disk. In the following the observable phenomena are discussed. The outer parts absorb the hard X-ray radiation and reemit the absorbed energy in the ultraviolet and optical wavelength range. This ultraviolet luminosity, in turn, can lead to the formation of a Strömgren sphere.[21] If the accretion increases, the luminosity will grow linearly and cause a raise of the effective temperature of the radiation, Figures 4.4 and 4.5.

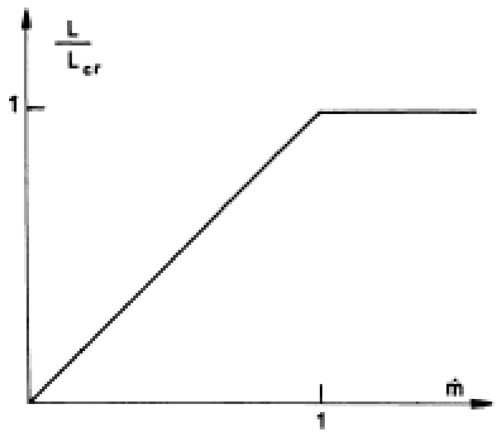

Figure 4.4: Luminosity of the disk around a collapsar (i.e. a collapsed stellar mass object) as a function of the matter flux entering its external boundary. (Shakura and Sunyaev 1973, p. 340)

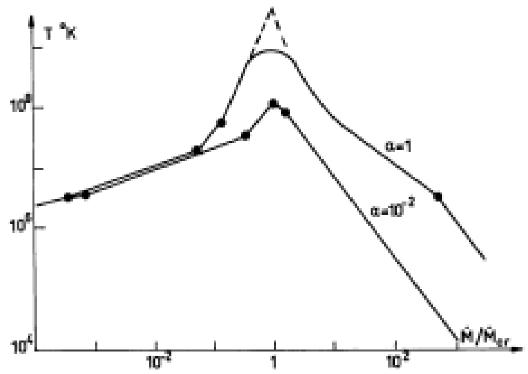

Figure 4.5: Dependence of the effective temperature of the radiation of the disk on the matter flux in it for different values of α. (Shakura and Sunyaev 1973, p. 340)

Another scenario would be the evaporation of the outer layers of the disk by the heating up due to the hard radiation. This would cause a decrease in matter flux into the black hole and influences its luminosity, as fluctuations of the disk's brightness are connected with the variability of the infalling matter flux. An unusual optical appearance may occur if the X-ray radiation of the black hole hits the surface of the stellar companion. Moreover, there might be a periodic variability of the luminosity due to the companion's movement around the black hole, as the distance of the two objects varies during the orbit. Eclipses of the radiation from the central object by the disk are expected if the plane of the disk does not coincide with the plane of the rotation of the system. A strong anisotropic behavior of matter outflow can be observed, when hot plasma is ejected with high velocity in a narrow cone. This hot, outflowing matter becomes opaque in the radio range far from the binary system. Also the appearance of non-thermal radiation mechanisms connected with the existence of magnetic fields and beams of fast outflowing particles are discussed. Finally, the most characteristic property of black holes in close binaries is the spectrum of the X-ray radiation. (Shakura and Sunyaev 1973)

4.3 Different Types of Accretion onto Black Holes

4.3.1 Subcritical Accretion

This subsection is based on the work of Shakura and Sunyaev 1973.
In the case of subcritical inflow of matter through the Roche lobe most of the matter is accreted. The

[21] The ultraviolet radiation is able to ionize the neutral hydrogen. This ionization is followed by recombination processes and a reemission of the energy as series of photons of less energy. This would form out a typical sphere, which is also formed by hot stars. However, those formed by hot stars are smaller for a similar optical luminosity. Therefore this sphere would distinguish a black hole from normal optical stars.

formation of the disk and the underlying mechanism of angular momentum transport are comparable with the ones introduced in Accretion Disks. In a disk around a black hole general relativity has to be taken into account at $R < 3R_g$. We defined $R_0 = 3R_g$ as the inner boundary of the disk (Figure 4.3). In the region where $R < R_0$ the matter falls without any externally observable effect. There would be an energy release per unit mass of infalling matter of $0.06c^2$, see $\eta_{\text{eff}} \simeq 0,06$ in 4.2.1, which leads to a total resulting luminosity of $L_0 = 0.06c^2\dot{M}$. At this particular accretion rate almost all of the angular momentum is transported outwards and only a small fraction falls together with the matter into the black hole. In the case of a non-rotating black hole, the energy flux from a surface unit increases when approaching the collapsar and reaches its maximum at $R = 1.36R_0$ (Figure 4.3). Considering the case of a rotating black hole, the released gravitational energy is transferred mechanically from the relativistic region $1/2R_g < R < 3R_g$ into a non-relativistic one $R > 3R_g$ and dissipates there. The disk, formed through an subcritical accretion, is considered to be composed of different parts.[22] These are shown for a better understanding in Figure 4.6.

a) $P_\mathrm{r} > P_\mathrm{g}$ and $\sigma_\mathrm{T} > \sigma_\mathrm{ff}$
In this region the radiation pressure dominates and the electron scattering on free electrons plays the major role in the interaction of matter and radiation and dominates the opacity. This part is located in the region of the maximal energy flux at $R = 1.36R_0$. In this region the disk has a constant thickness along the radius. The height depends on the value of accretion rate. The maximal ratio $z_0/R = \dot{m}$ is reached at $r = R/3R_\mathrm{g} = 2.25$, with $z_0 = c_s/v_\phi R$ the half thickness. The temperature of the plasma inside the disk can be defined as $T = 2.3 \cdot 10^7(\alpha m)^{-1/4} r^{-3/4}\mathrm{K}$. A „true“ optical depth of $\tau^* = 8.4 \cdot 10^{-5}\alpha^{-17/16} m^{-/16}\dot{m}^{-2} \cdot r^{-93/32}(1 - r^{-1/2})^{-2}$ is determined. The disk is thus opaque ($\tau^* > 1$) if $r > 25\alpha^{34/93}\dot{m}^{64/93}m^{2/93}(1 - r^{-1/2})^{64/93}$, which justifies the assumption of local thermodynamical equilibrium. This local thermodynamical equilibrium exists inside the disk up to $R \approx 10R_0$. There exists a limitation of energy losses through radiation of the plasma due to the low production rate of photons by free-free processes. However, the energy loss is increased by comptonization of the low frequency radiation, which causes as well a decrease in the plasma temperature.

b) $P_\mathrm{g} \gg P_\mathrm{r}$ and $\sigma_\mathrm{T} > \sigma_\mathrm{ff}$
In the adjacent part of the disk the pressure is dominated by the gas pressure. The main contribution to the opacity is again the electron scattering. The values for the temperature as well as for the optical depth are given here for completeness: $T = 3.1 \cdot 10^8 \alpha^{-1/5}\dot{m}^{2/5}m^{-1/5}r^{-9/10}(1 - r^{1/2})^{2/5}$ and $\tau^* = 10^2\alpha^{-4/5}\dot{m}^{9/10}m^{1/5}r^{3/20}(1 - r^{-1/2})^{9/10}$. One can find a boundary radius between region *a*) and *b*):

$$\frac{r_{ab}}{(1 - r_{ab}^{-1/2})^{16/21}} = 150(\alpha m)^{2/21}\dot{m}^{16/21} \tag{4.4}$$

which in turn tells us that region *a*) only exists if $\dot{m} \gtrsim 1/170(\alpha m)^{-1/8}$.

c) $P_\mathrm{r} \ll P_\mathrm{g}$ and $\sigma_\mathrm{ff} > \sigma_\mathrm{T}$
The last part is the outermost region. Here again the gas pressure dominates, but the opacity is determined by the free-free absorption. One finds $T = 8.6 \cdot 10^7 \alpha^{-1/5}\dot{m}^{3/10}m^{-1/5}r^{-3/4}(1 - r^{-1/2})^{3/10}$ and $\tau \propto \sigma_\mathrm{ff} = 3.4 \cdot 10^2\alpha^{-4/5}\dot{m}^{1/5}m^{1/5}(1 - r^{-1/2})^{1/5}$. If α decreases, the surface density increases rapidly, which reduces the radial velocity of motion. In turn, the disk's thickness grows only as $\alpha^{-1/10}$. In this regime the disk is always opaque.

Again a boundary radius between the regions *b*) and *c*) can be determined as

$$r_{bc} = 6.3 \cdot 10^3\dot{m}^{2/3}(1 - r_{bc}^{-1/2})^{2/3}\ , \tag{4.5}$$

[22] In some equations of the explanation of the distinguished parts, dimensionless parameters are used: $m = M/M_\odot$, $\dot{m} = \dot{M}/\dot{M}_\mathrm{crit}$, $r = R/3R_\mathrm{g}$. σ_T represents the opacity due to Thompson scattering, the photon scattering on free electrons, and σ_ff the opacity due to the free-free absorption.

which is valid in the case $v_r \ll \Omega$ and only if $r - 1 > 10^{-6}\alpha^{8/7}\dot{m}^{3/7}$.

Finally, it has to be mentioned that disk accretion is feasible at sufficiently weak turbulence and a weak magnetic field. Determining the structure of the disk along the z-coordinate, one finds that the pressure gradient balances the component of the gravitational attraction perpendicular to the disk plane. Therefore, hydrostatic equilibrium exists in the direction perpendicular to the disk plane. The disk's structure is characterized by the temperature of the mid-plane that depends only on R.

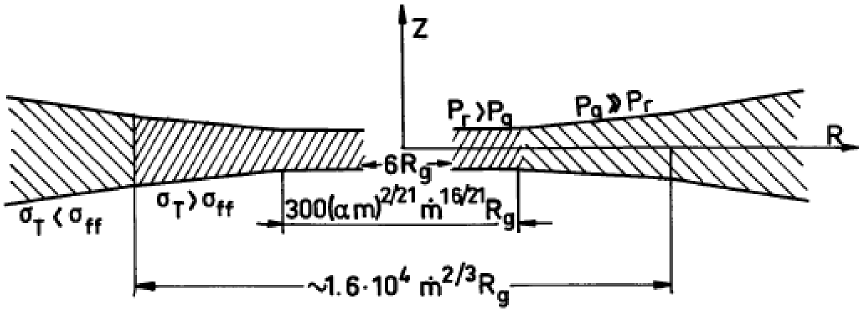

Figure 4.6: Illustration of the different regions of a disk with subcritical accretion. (Shakura and Sunyaev 1973, p. 347)

The local spectrum of the thermal radiation is likely to be one of the spectra of the three above distinguished parts. A Planck distribution in the outer parts of the disk, a Wien distribution in the inner region and in the intermediate region a spectrum of radiation that has passed through the medium with electron scattering. In the inner part the spectrum is strongly affected by the processes of comptonization. The spectra of a) the outer disk, b) and c) the intermediate region and d) the inner disk are shown in Figure 4.7. The surface temperature of matter as a function of radius is presented in Figure 4.8.

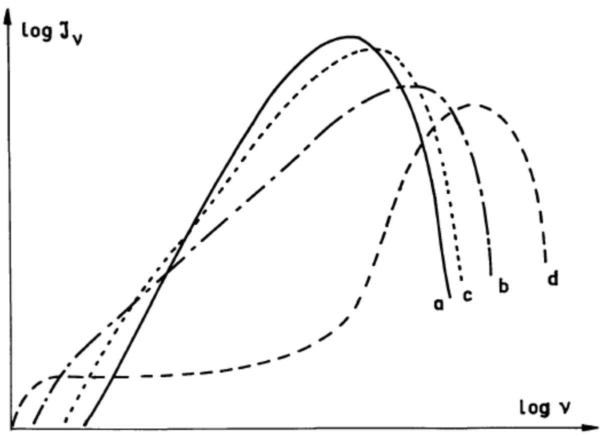

Figure 4.7: Typical distributions of radiation formed in the disk: a) the black body spectrum, b) the radiation spectrum of an isothermic, homogeneous medium, c) the radiation spectrum of an isothermal, exponential atmosphere (the main contribution to the opacity in b) and c) comes from electron scattering) and d) the spectrum formed as a result of comptonization
(Shakura and Sunyaev 1973, p. 339)

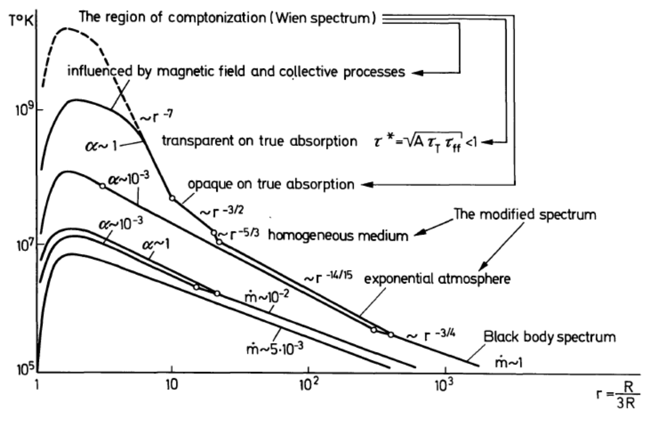

Figure 4.8: Distribution of the surface temperature along the radius of the disk for different $\dot{M}$ and α.(Shakura and Sunyaev 1973, p. 349)

4.3.2 Super Eddington Accretion

This subsection is based on the work of Shakura and Sunyaev 1973. Assuming the case of supercritical accretion, the region around the black hole, its environment, respectively, may become observable. In this supercritical regime, where $\dot{M} \gg 3 \cdot 10^{-8} M_{\odot}/\mathrm{year}$, the luminosity is stabilized at the critical limit of $L \approx 10^{38} M/M_{\odot}$ erg/s. An outflow of matter due to the radiation pressure is formed. The major part of the matter flows out with high velocities. The density of the outflowing matter depends on the efficiency α of mechanism of angular momentum transport and is a function of $\dot{M}/\dot{M}_{\mathrm{crit}}$. This density determines the electromagnetic spectrum of the outflow. Analyzing the spectrum one finds that most of the energy is radiated in the ultraviolet and optical range of the spectrum. Moreover, it is conspicuous that in the upper layers of the outflowing matter broad emission lines are formed. The outflow begins close to the radius where the radiation pressure and gravitation pressure are comparable. Just a small fraction, the critical flux of matter, falls under the gravitational radius and is accreted. The accreted matter and the one ejected is opaque for the emitted radiation and therefore influences the spectrum. At the supercritical state the black hole may appear as a bright, hot, luminous star with a large outflow of mass. The velocities of the mass outflow are around $v \sim \alpha \cdot 10^5 (\dot{M}_{crit}/\dot{M})^{1/2}$ km/s. The central black hole is surrounded by a cooler disk and the matter, as a consequence of accretion, enters the collapsar. Consequently, the structure and the radiation spectrum depends significantly on the inward and outward mass flux. The critical regime corresponds again with the Eddington accretion rate and luminosity as calculated in the Introduction. (Shakura and Sunyaev 1973) In other words and using again the definition of the trapping radius, one could say that r_t moves out (Spruit 1996a).

In the following we will discuss the case of supercritical accretion in more detail and quantify the former estimations with some equations. These equations and the discussion is based on the work of Shakura and Sunyaev 1973.

Considering the critical Eddington luminosity, the radiation pressure on the electrons is comparable with the gravitational attraction of protons and nuclei. Consequently, the flux of matter can not exceed $\dot{M}_{\mathrm{crit}} = L_{\mathrm{E}}/\eta c^2$. One characteristic of disk accretion is the narrow region of matter infall. The movement of the matter is in fact a slowly twisting spiral in the plane perpendicular to the direction of the angular momentum of the matter flowing into the disk. The energy release in the disk, during processes of angular momentum transport, is proportional to $R^{-3}[1-(R_o/R)^{1/2}]$. In the outer regions a qualitative difference between the subcritical and the supercritical accretion can not be found. The energy release here is less than the critical luminosity and the radiation pressure does not prevent infall of the matter along the disk.

Some modifications of the description of the supercritical accretion are suggested, like a periodic sequence of supercritical fluxes of matter and a destruction of the whole disk by powerful flares of radiation. Moreover, a stationary state with the luminosity close to the critical value and with an outflow of most of the matter beyond the system seems to be likely. In this case the energy release as well as the force of radiation pressure grow rapidly when getting closer to the black hole. If $\dot{m} = \dot{M}/\dot{M}_{\mathrm{crit}} > 1$, the thickness of the disk becomes of the order of the distance to the black hole near the radius of spherization[23] $R_{sp} \approx 9/4 \cdot 10^6 m\dot{m}$[cm]. In this scenario the infall of matter would lead to an immediate outflow of a fraction of it from the region $R < R_{sp}$. The difference of the forces of gravitational attraction and radiation pressure causes an acceleration of the outflowing matter. The velocity of the outflow can be determined as $v_{\mathrm{out}} \simeq \sqrt{2}v_\phi\sqrt{(L - L_{\mathrm{E}})/L_{\mathrm{E}}}$, which is close to the radial velocity of the matter in the central plane of the disk $v_{\mathrm{r}} = \alpha v_\phi(R_s)$. A decrease of v_{out} increases the luminosity and in turn the velocity of the outflowing matter. On the other hand, if v_{out} exceeds v_{r}, the luminosity and the matter inflow to the region $R < R_{\mathrm{sp}}$ decrease, which decreases in turn v_{out}. The lines of matter flow are illustrated in Figure 4.9 and the matter outflow in spirals is shown in Figure 4.10. The closer the matter comes to the black hole, the greater is the outflowing velocity. As angular momentum is conserved, it is not possible for matter to enter the region with a radius less than the radius of the outflow. Due to this a small cone of hot matter with high velocity and hard X-ray radiation at an opening angle θ relative to the axis of the disk rotation is ejected from the region $R \sim 9/4R_0 \sim 7R_{\mathrm{g}}$. With an increase of θ a decrease of the velocity of the outflowing matter is related. The emitted spectrum is dependent on the parameter α, the rate of matter inflow to the disk and the absorption and reemission of the hard radiation. Considering $\dot{m} \gg 1$ and $\alpha(r_{\mathrm{sp}}) \ll 1$ the matter may be opaque far from the object. Consequently, the collapsar appears for $\dot{m} > 3 \cdot 10^3(\alpha/m)^{2/3}$ as a bright optical and ultraviolet object with high mass loss and possible X-ray radiation.

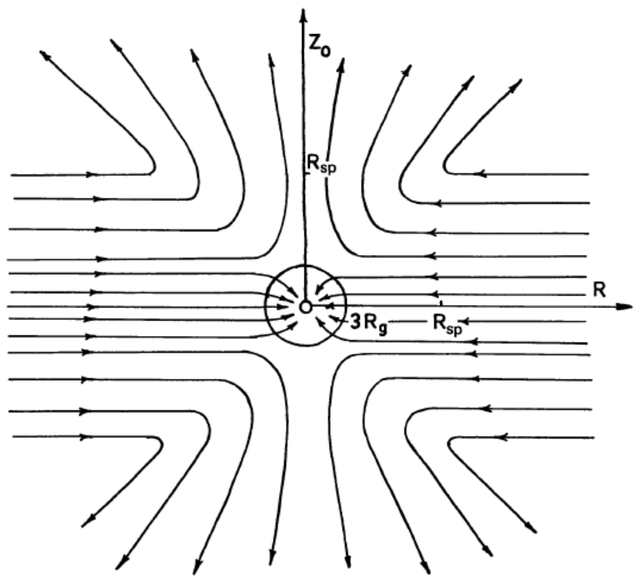

Figure 4.9: Lines of matter flow in the case of supercritical accretion: For $R < R_{\mathrm{sp}}$ spherization takes place, which initiates matter outflow from the collapsar (Shakura and Sunyaev 1973, p. 347).

[23] The spherization radius R_{sp} is a critical radius inside which quasi-spherical outflows emerges, $R_{\mathrm{sp}} = (\dot{M}c^2/L_{\mathrm{E}})R_*$.

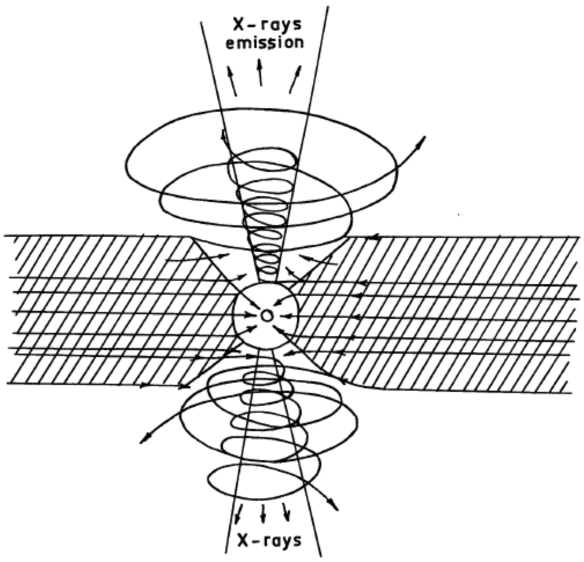

Figure 4.10: Outflow of the matter from the black hole in a spiral (Shakura and Sunyaev 1973, p. 347).

4.3.3 Ion Supported Accretion Flows

An accretion flow is defined as an ion supported accretion flow (ISAF) in the case that the thermal equilibrium between ions and electrons breaks down and a two temperature plasma forms. This kind of flows occur when the gas is optically thin and radiation processes are inefficient. Considering this case, the gas heats up near the virial temperature. At the last stable orbit of a black hole this would yield to a temperature of $\sim 10^{12}$K, or 100MeV. In this considerations the viscous dissipation energy is distributed equally to all the carriers of mass by the radiation. Due to the bigger mass of the ions they hold most of the energy, whereas only $\sim 1/2000$ resides in the electrons. The high mass of ions prevent them from the rapid acceleration needed for the emission of electromagnetic waves and so their radiation is weak. The energy is transferred through Coulomb interactions to the electrons. This is a slow process, because of the low density and the decrease of their interaction with the electrons with increasing temperature. Based on the basic definition of a plasma the electric forces for the transfer act only as long as the ion is within the electron's Debye sphere. Consequently, the flow is characterized by a two-temperature state, with ions near the virial temperature and a much lower temperature, $50 - 200$keV, for the electrons that are responsible for the radiation. So we have a fast energy transfer from the gravitational field to the ions, a slow transfer from the ions to the electrons and once again a fast emission from the electrons. Therefore such a flow is radiatively inefficient as the carriers of the accretion energy, the ions, will be swallowed by the central mass before the transfer of the energy can take place. Most of the energy will be accreted with the infalling matter. The efficiency of radiation is suggested to be $\eta \ll 0.1$ for a cool disk. Thus the physics of the flow as well as the observed spectrum is mostly determined by the ion-electron interaction. Many uncertainties with regard to ISAF's remain still open as this theory is mainly dependent on some properties of the disk, such as the strength of the magnetic field, that are not clarified yet. Ion-supported accretion flows require low densities, that occur either because of low accretion rates or high values of α. The fact that the time for the energy transfer of ions is longer than the accretion time, yields to a maximum accretion rate $\dot{m} \leq \alpha^2$. Inserting the probable value of $\alpha = 0.05$, the accretion rate would be a few $10^{-3} M_\odot$ per year. For systems with higher accretion rates, a bigger value of α would be necessary to develop ISAFs. (Spruit 1996a)

4.4 Observation on Saggitarius A*

The following discussion is based on the paper of M. Zamaninasab 2010.
The nearest SMBH is the center of our Galaxy, Saggitarius A*, with a luminosity of $10^{-9} - 10^{-10} L_{\mathrm{Edd}}$. It is one of the most extreme sub-Eddington sources available for observations. Near-infrared (NIR) and X-ray flares have been detected with high spatial and spectral resolution observations. These outbursts last usually for about 100 min and appear four to five times a day. Images of Saggitarius A* are shown in Figure 4.11. Due to the small time scale of the variations of the NIR and X-ray flares, the region of emission is suggested not to be bigger than 10 Schwarzschild radii of the SMBH. Furthermore, the high polarization of the NIR flares favours as responsible radiation mechanism synchrotron-self-compton (SSC) or inverse Compton emission. The short periods of increased radiation seem to be correlated to quasi-periodic oscillations (QPOs). This quasi-periodicity, in turn, has been suggested to be related to the orbital time scale of the matter in the inner regions of the disk. Furthermore, the existence of a correlation between the modulations of the observed flux density light curves and the changes in polarimetric measurements is tried to be probed and explained.
Different models for explaining the outbursts have been taken into account. The favoured and in the paper discussed model is the so-called Emission Model, in which the main flare is caused by a local perturbation close to the marginal stable orbit of the black hole. Perturbations can originate in magnetic reconnections, stochastic acceleration of electrons due to magneto hydrodynamical (MHD) waves, magneto-rotational instabilities (MRI) etc. A schematic view of the geometry of the model is given in Figure 4.12. Due to the spreading of these instabilities, a temporary bright torus around the black hole is produced. The mentioned variability is are mainly generated, in this model, through relativistic flux modulations caused by an azimuthal asymmetry in the torus. Since all these processes happen close to the black hole and therefore in a very strong gravitational regime, relativistic effects have to be taken into account. For the modeling of the data a special ray-tracing code has been used that is able to calculate all the effects of general relativity, such as light bending, gravitational lensing, redshift and Doppler boosting etc. In the work of M. Zamaninasab 2010 various images have been simulated that an observer for different inclinations with respect to the accretion disk would measure. (For more detailed information and all modeled light curves and images see M. Zamaninasab 2010).
The question arises how a spot can survive long enough to be responsible for the flux modulations four to five times a day. One possible answer might be that the sub-mm seed photons are up-scattered to the NIR and X-ray frequencies due to a SSC mechanism. The mechanism for stabilizing such a spot remain unknown. However, the existence of persistent vortices in accretion disks might be a possibility. The pattern recognition analysis showed that strong lensing patterns are detectable in the observed NIR light curves. This in turn, is a further indicator for a (clumpy) accretion disk around Sgr A*. Additional simulations have shown that an orbiting spot is able to produce the same cross correlation pattern as observed, but the orbital frequency will be mainly a quasi-periodic signal. Moreover, a spotted accretion disk has been modeled, where spots are born, evolve and fade away with time, distributed in a narrow belt, $1 - 2 \cdot r_{\mathrm{ISCO}}$[24], of the accretion disk. It has been found that the kind of observed correlation between the flux and the polarization data can not be produced by random processes, which emphasizes again the existence of orbiting matter around the black hole.
Conclusively, it can be said that a general relativistic simulation of turbulences in the inner parts of the accretion disk fits the observed behavior of Sgr A*. Alternative models could produce the same observed phenomena, for instance shocks in relativistic jets could produce correlated total and polarized fluxes. Under certain circumstances a relativistic flux would be able to produce the same correlation and the observed patterns. The changes in the observed polarization angle simultaneous to the flux magnification and changes in the degree of the NIR polarization support the idea of a geometrical shape dominated by compact azimuthal asymmetries. Moreover, a toroidal magnetic field structure seems to fit best data deduced from observations.

[24] r_{ISCO} refers to the radius of the marginal stable orbit, also called the ISCO as introduced in former sections.

To sum up, many of the measured data support the theory of accretion disks, some kind of matter surrounding the black hole in the middle of our Galaxy, respectively. The correlation between changes in the polarimetric data and total flux densities, which indicate strong gravity effects, provides evidence that the variations may originate from the inner parts of the accretion disk. For explaining the behavior of Sgr A* many models are suggested. Some of them are not able to give answers for important questions, whereas the hot spot model seems to give reasonable results and fits the observations very well. Understanding the underlying processes would be a big achievement in the field of research of accretion disks and their evolution. As there remain many phenomena uncertain, this subject of physics will provide work for further decades.

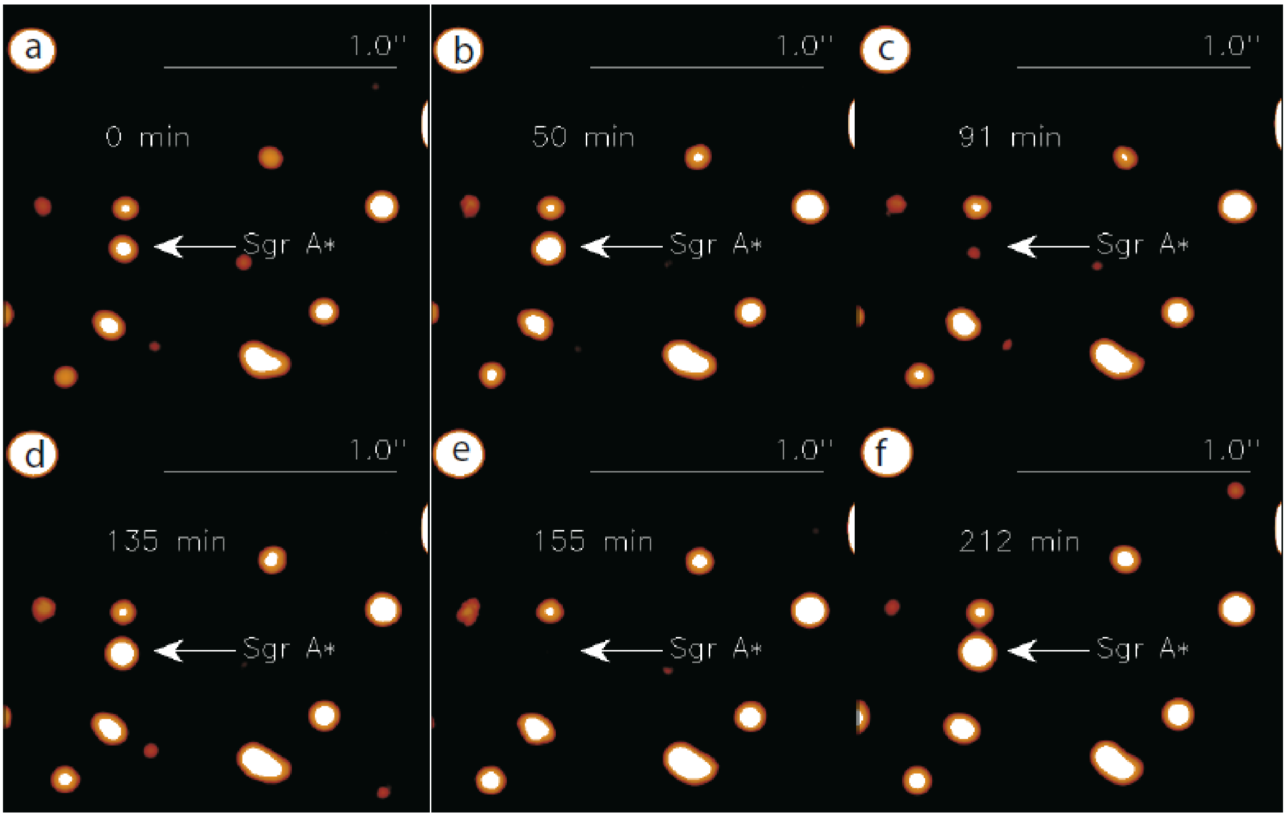

Figure 4.11: Observations of Saggitarius A*: Images observed in the NIR L'-band (3.8 μm) on 3 June 2008 between 05:29:00 and 09:42:00 (UT time). The images a-f show Sgr A* 0, 50, 91, 135, 155 and 212 min after the start of observations. In its flaring state the flux changes up to 100% in time intervals of the order of only tens of minutes. (M. Zamaninasab 2010, p. 2)

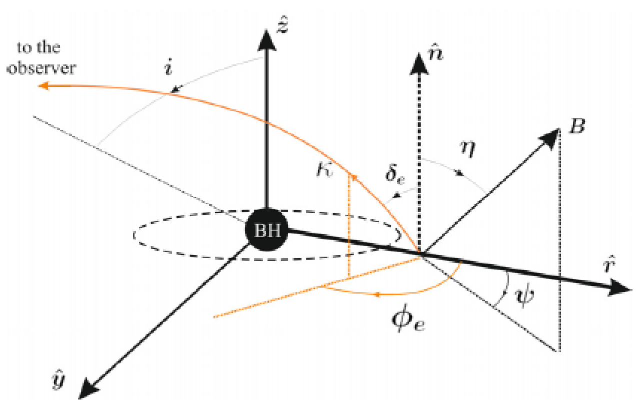

Figure 4.12: Geometry of the Emission Model for Saggitarius A*: The accretion disk lies on the $\hat{\mathbf{y}}$ - $\hat{\mathbf{r}}$ plane, where $\hat{\mathbf{n}}$ represents the unit normal vector of the disk. The magnetic field lines are B, their direction is defined by the two angles η and ψ. The direction of the momentum of the emitted photon κ is as well determined by two angles, δ_c and ϕ_c. The inclination of the line of sight of an observer is i. (M. Zamaninasab 2010, p. 11)

Physical Quantities

ϕ	point like potential
ΔE	kinetic energy
G	gravitational constant
M	central objects mass
M_{BH}	mass black hole
r	radius, distance from the center
e	dissipated energy/internal energy
γ	ration of the specific heat
P	pressure
P_{tot}	total pressure
P_r	radiation pressure
P_g	gas pressure
∇P	pressure gradiant
$\mathcal{R}$	universal gas constant
T	temperature of the gas
T_{vir}	virial temperature
T_{c}	central temperature
T_{g}	gas temperature
T_{d}	dust temperature
T_{BL}	boundary layer temperature
μ	mean atomic weight per particle
ρ	density
c_{s}	speed of sound
τ_{d}	dynamical or free fall time scale
τ_{visc}	viscous/secular time scale
τ_{acc}	accreting time scale
τ_{therm}	thermal time scale
τ_{c}	cooling time scale
τ_{h}	heating time scale
τ	optical depth
v_{k}	Keplerian orbital velocity
v_{r}	radial or „drift“velocity
v_{out}	velocity of outflow
v_{esc}	escape speed
Ω_{k}	Keplerian angular velocity
Ω	angular velocity
$\dot{M}$	accretion rate
$\dot{M}_{\mathrm{E}}$	Eddington accretion rate
F	radiative flux
F_{E}	Eddington flux
L_{E}	Eddington luminosity
L_{LB}	boundary layer luminosity
c	speed of light
$M_{\odot}$	mass of the sun
$L_{\odot}$	luminosity of the sun

(r, ϕ, z)	cylindrical polar coordinates
$\hat{\mathbf{r}}$	unit vector in the spherical radial direction
g_{z}	residual acceleration towards the midplane
$\rho_0(r)$	density at the midplane
l	specific angular momentum
$\mathbf{T}$	torque
$H(r)$	scale height, disks thickness
r_{t}	trapping radius
η_{eff}	efficiency of gravitational energy release
z	z direction perpendicular to the disk's plane
δ	aspect ratio of the disk
$\mathbf{v}$	velocity
Σ	surface density
ν	turbulent viscosity
Ω'	derivation of the angular velocity of disk rotation with respect to r
$Q(r)$	energy dissipation rate
Re	Reynoldsnumber
n	number density of molecules
σ	cross-section
λ_{t}	size of the turbulent eddies
v_{t}	turnover velocity
α	α-parameter
q^{-}_{thick}	radiative emission rate, optical thick case
q^{-}_{brak}	thermal braking radiation
q^{+}	viscous dissipation rate
q^{-}	radiative loss rate
q_{adv}	net energy advection rate per unit volume
λ	mean free path or wavelength
$\tilde{r},\ \tilde{t}$	dimensionless parameters
σ_{SB}	Stefan-Boltzmann's constant
σ_{ff}	opacity determined by free-free absorption
σ_{T}	opacity determined by electron scattering
$f(r)$	heat factor
S	entropy per unit mass
F	energy/heat flux
$T_{\mathrm{s}}(r)$	surface temperature
r_{*}	stellar radius
T_{*}	temperature of the inner disk, stellar temperature
ϑ	frequency
ϕ	angle of inclination
I_{θ}	emitted spectrum
B_{θ}	Planck function
S_{ϑ}	flux at frequency ϑ
r_{out}	outer radius
k	Boltzmann's constant
r_{i}	inner radius of the disk
β	parameter
E_{t}	enthalpy of disk per unit of suface area
W_{visc}	heating rate
W_{grav}	gravitational energy release
$\dot{m}$	dimensionless value

E	energy density
κ	scattering/absorbing surface area or opacity
h	half thickness, special angular momentum, Planck's constant
a	radiation density constant in σ_{SB}, separation
V_{eff}	effective potential
$\phi_{\mathrm{R}}(\mathbf{r})$	Roche potential
$\dot{J}$	angular momentum flux
R_{g}	gravitational radius, Schwarzschild radius
R_{sp}	radius of spherization
i	inclination angle
θ	angle relative to the disks axis
r_{crit}	critical point

Bibliography

Alecian, E. (2013). “An Introduction to Accretion Disks”. In: *Lecture Notes in Physics 857*, pp. 183–205. DOI: 10.1007/978-3-642-30648-_7.

Asmus, Daniel (2008). “Der Innere Rand von Akkretionsscheiben um Schwarze Löcher”. MA thesis. Christian-Albrechts-Universität zu Kiel.

C.P. Dullemond D. Hollenbach, I. Kamp and P. D’Alessio (2006). “Models of the structure and Evolution of protoplanetary Disks”. In: *Astro-ph/0602619v1*.

Hawking, Stephen (2001). *Das Universum in der Nussschale*. Ed. by Hoffmann und Campe. Hoffmann und Campe.

Juhan Frank, Andrew Kind and Derek Raine (2002). *Accretion Power in Astrophysics*. Ed. by Cambridge University Press. Third Edition. The Press Syndicate of the University of Cambridge.

Kato, Y. and K. Shibata S. Mineshige (2004). “Magnetohydrodynamic Accretion Flows: Formation of Magnetic Tower Jet and Sunsequent Quasi-Steady State”. In: *The Astrophysical Journal 605*, pp. 307–320.

Kenyon, S. J. and L. Hartmann (1987). “Spectral Energy Distribution of T Tauri Stars: Disk Flaring and Limits on Accretion”. In: *The Astrophysical Journal* 323, pp. 714–733.

Kraus, Michaela (2003). “SEDs of flared dust disks: radiation transfer model versus two-layer model”. In: *Astro-ph/0305532*.

Lynden-Bell, D. (2002). “Why do disks form Jets?” In: *ASP Conference Series* 249. Institute of Astronomy, Cambridge; UK.

Lynden-Bell, D. and J.E. Pringle (1974). “The Evolution of viscous discs and the origin of the nebular variables”. In: *Monthly Notices of the Royal Astronomical Society 168*, pp. 603–637.

M. Zamaninasab, A. Eckart et. al. (2010). “Near infrared flares of Sagittarius A*”. In: *Astronomy and Astrophysics* 510 A3. DOI: 10.1051/0004-6361/200912473.

Mamatsashvili, George (2011). “Angular Momentum transport in accretion discs”. MA thesis. Institute for Astronomy, University of Edinburgh.

Müller, Dr. Andreas (2010). *Schwarze Löcher*. Ed. by Springer. Spektrum Akademischer Verlag.

Narayan, Ramesh and Robert Popham (1994). “Theory of Accretion Disks - 2”. In: ed. by Kluwer Academic Publishers. Vol. 417. NATO ASI Series 1389-2185. Springer Netherlands. Chap. Accretion Disk Boundary Layers, pp. 293–307. DOI: 10.1007/978-94-011-0858-4_30.

Narayan, Ramesh and Insu Yi (1994). “Advection-Dominated Accretion: A self-similar solution”. In: *The Astrophysical Journal 428*, pp. L13–L16.

Ogilvie, G. I. (1999). “The non-linear fluid dynamics of a warped accretion disc”. In: *Monthly Notices of the Royal Astronomical Society* 304, pp. 557–578. DOI: 10.1046/j.1365-8711.1999.02340.x.

Shakura, N.I. and R.A. Sunyaev (1973). “Black Holes in Binary Systems. Observational Appearance”. In: *Astronomy and Astrophysics 24*, pp. 337–355.

Spruit, H.C. (1996a). *Accretion Disks*. Tech. rep. Max-Planck- Institut für Astrophysik.

– (1996b). “Magnetohydrodynamic Jets and Winds from Accretion Disks”. Max-Planck-Institut für Astrophysik.

– (2010). “Theory of magnetically powered jets”. In: *Lecture Notes in Physics794*, pp. 233–263.

Thorne, Kip S. (1994). *Black Holes and Time Warps*. W. W. Norton & Company, Inc.